OAR RESEARCH REVIEW

OFFICE OF AEROSPACE RESEARCH ★ UNITED STATES AIR FORCE

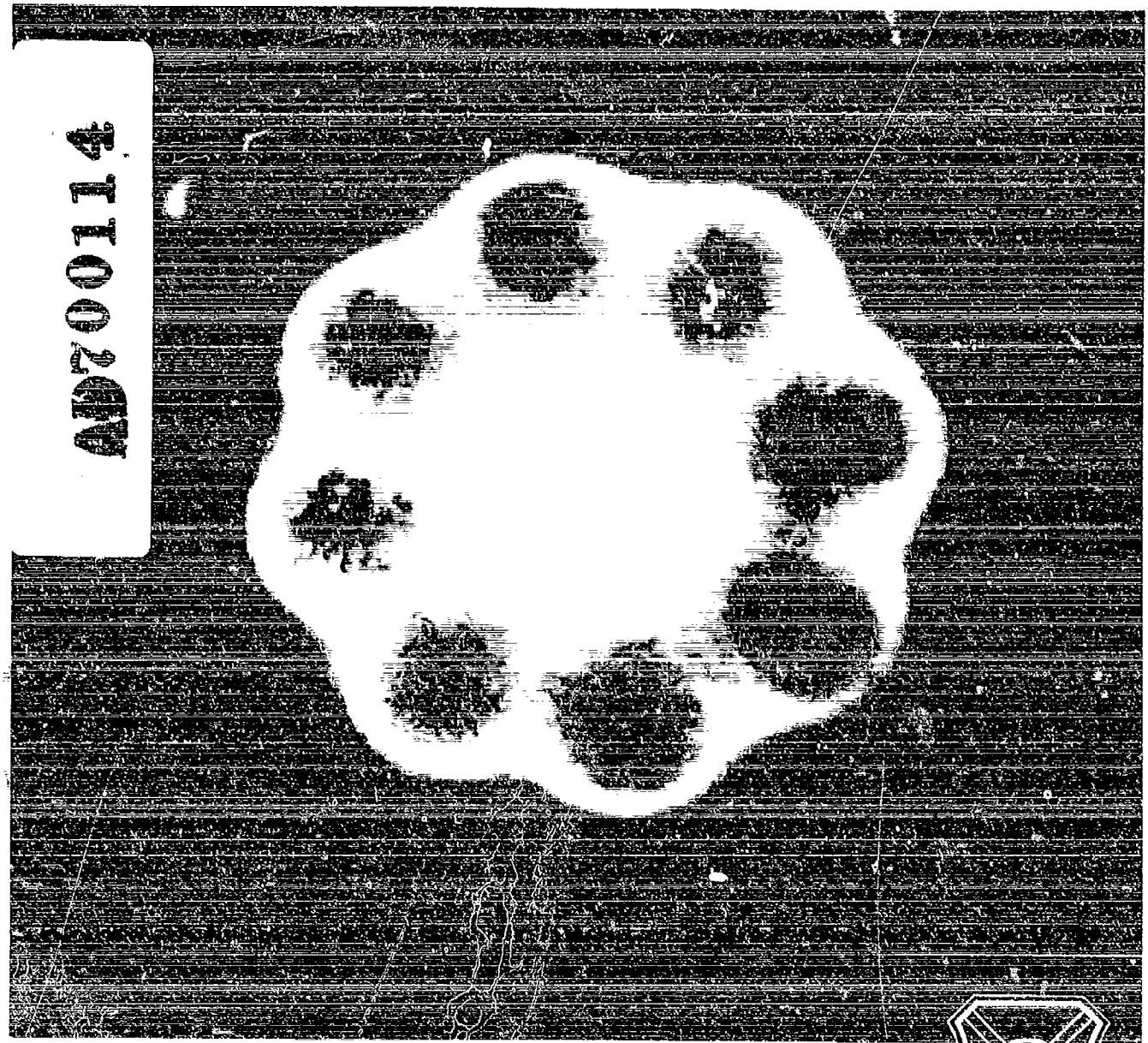

OAR: The Research Agency of the United States Air Force

Volume IX, Number 1 January-February 1970

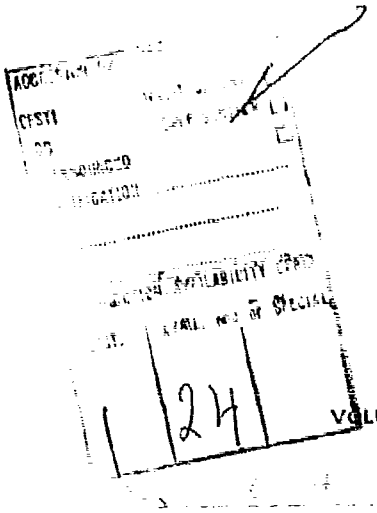

OAR RESEARCH REVIEW

VOLUME IX NUMBER 1 Jan-Feb 1970

ON THE COVER:

In this photo, the resonance pattern of a device that emits electromagnetic radiation is made visible for the first time. The areas of most intense radiation are the lighter areas. These patterns can be readily changed by varying the excitation frequency.

The pattern is made visible by using a detector fabricated from liquid crystals. The resonator itself is a small ceramic disc about one inch in diameter. (See article in this issue, "Color Display of Resonance Patterns.")

OAR RESEARCH REVIEW is published bimonthly by the Directorate of R&D Interactions (PGR), HQ Office of Aerospace Research, USAF, 1400 Wilson Boulevard, Arlington, Va. 22209. The objective of this publication is to make a positive contribution to the exchange of information concerning Air Force conducted and sponsored research activities.

JACOB SEIDEN *Editor*

For sale by the Superintendent of Documents, U.S. Government Printing Office, Washington, D.C. 20402 – $3.00 per year domestic, 75 cents additional for foreign mailing, 45 cents per single copy and 30 cents per Annual Index. Back issues will not be furnished.

MICROWAVE PHYSICS LABORATORY, AFCRL

color display of resonance patterns

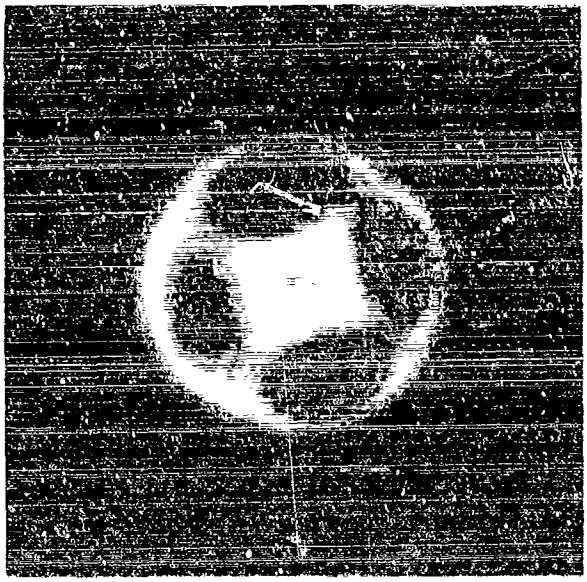

Figure 1. This photo shows a visible resonance pattern from the same disc as the one referred to in the caption for the cover photo; however, the resonance pattern is somewhat different. (See caption for the cover photo).

A quick and simple method for measuring the resonance patterns of dielectric resonators a method using liquid crystals—has been demonstrated by James C. Sethares and Martin R. Stiglitz of AFCRL. Resonance patterns, or modes, of a resonator are presented on a detector as a visual picture in color. What is seen—and seen for the first time—are the specific areas within the total resonator material that vibrate and emit electromagnetic energy. Thus the sources of EM energy are pinpointed.

Resonators are used in electronic circuits as filters to extract a narrow band of frequencies from a broader spectrum. The detector that AFCRL has developed to study the emission patterns of resonators is uncomplicated: it looks something like a 35-mm glass-mounted slide and has no electrical or other connections. In operation, the detector plate is mounted close to the flat face of the resonator, leaving a gap of ⅛ inch or so.

Depending on the resonance mode, EM energy is emitted from different areas on the flat resonator surface. The mode pattern is projected across the gap to the detector where it is visibly mirrored. When the frequency used to excite the resonator is changed, the areas on the resonator surface that emit radiation also change.

The dominant frequency of the resonator is seen as a large darkened spot with gradations of color outward, indicating that the source of the EM emissions is centered on the face of the resonator. (See cover photo and Figure 1.) Various harmonics of this dominant frequency can be seen—depending on the excitation frequency—as two, four, six, eight, or more darkened areas arranged in geometrically symmetrical rosettes. Since mathematical calculations to obtain such mode patterns are prohibitively complex, they can only be approximated.

In addition to changes produced by different excitation frequencies, resonance patterns are strongly dependent on the physical configuration of the resonator. One resonator used by AFCRL in its study consisted of a small, flat ceramic disc slightly more than an inch in diameter and ½ inch thick. With this disc resonator, AFCRL has observed more than 25 different resonating patterns produced by exciting the resonator at different frequencies between 1.5 to 7 GHz.

The detector is a simple, three-layered plate, with liquid crystals comprising the center layer. These crystals, introduced only recently, have already had a range of applications discovered for them by researchers and manufacturers. They have the property of changing color with temperature. At 33°C, for example, they are red, with color changes being approximately linear through the spectrum until blue is observed at 37°C. As organic materials, they have a composition similar to that of cholesterol in the blood stream, and can be spread like paint.

The AFCRL detector can be fabricated in about 10 minutes. First, a liquid-crystal layer is spread on a resistive substrate layer. Then, the liquid-crystal layer is covered with a clear sheet of Mylar.

The conversion of EM-energy emissions from the resonator to the heat energy required to change the color of the liquid crystals is also straightforward. The electric-field component in the EM radiation from the resonator sets up

an electric current in the resistive layer. Resistive heating selectively raises the temperature at those points in the resistive layer that correspond to the points on the resonator emitting EM energy. This heats the overlaying liquid crystals, thus changing their color. Color changes persist in the detector for about a second after exposure to radiation. This process can be repeated hundreds of times before the crystals lose their sensitivity.

Mr. James C. Sethares is a research physicist in the Microwave Acoustics Branch of AFCRL's Microwave Physics Laboratory. He is at present concerned with experimental and theoretical investigations of spin-wave phonon interactions in single-crystal ferrites at microwave frequencies.

Mr. Sethares received his B.S. in Electrical Engineering from the University of Massachusetts in 1959, and his M.S. in Electrical Engineering from the Massachusetts Institute of Technology in 1962.

During the summers of 1959 and 1960, Mr. Sethares was employed by the Woods Hole Oceanographic Institute. He has also been a part-time Lecturer on Mathematics in the Department of Continuing Education at Boston University, a part-time teacher in the Department of Electrical Engineering at Lowell Technological Institute, and a full-time teaching assistant in the Department of Electrical Engineering at MIT.

Mr. Sethares is a member of RESA, IEEE, Tau Beta Pi, Sigma Xi, and Phi Kappa Phi, and has published a number of papers on his work.

Mr. Martin R. Stiglitz is an electronic engineer in the Microwave Acoustics Branch of AFCRL's Microwave Physics Laboratory. He is presently engaged in research on the interaction of EM waves and acoustic waves in solids. He received a B.B.A. in Engineering and Management from Northeastern University in 1959, and is a member of IEEE.

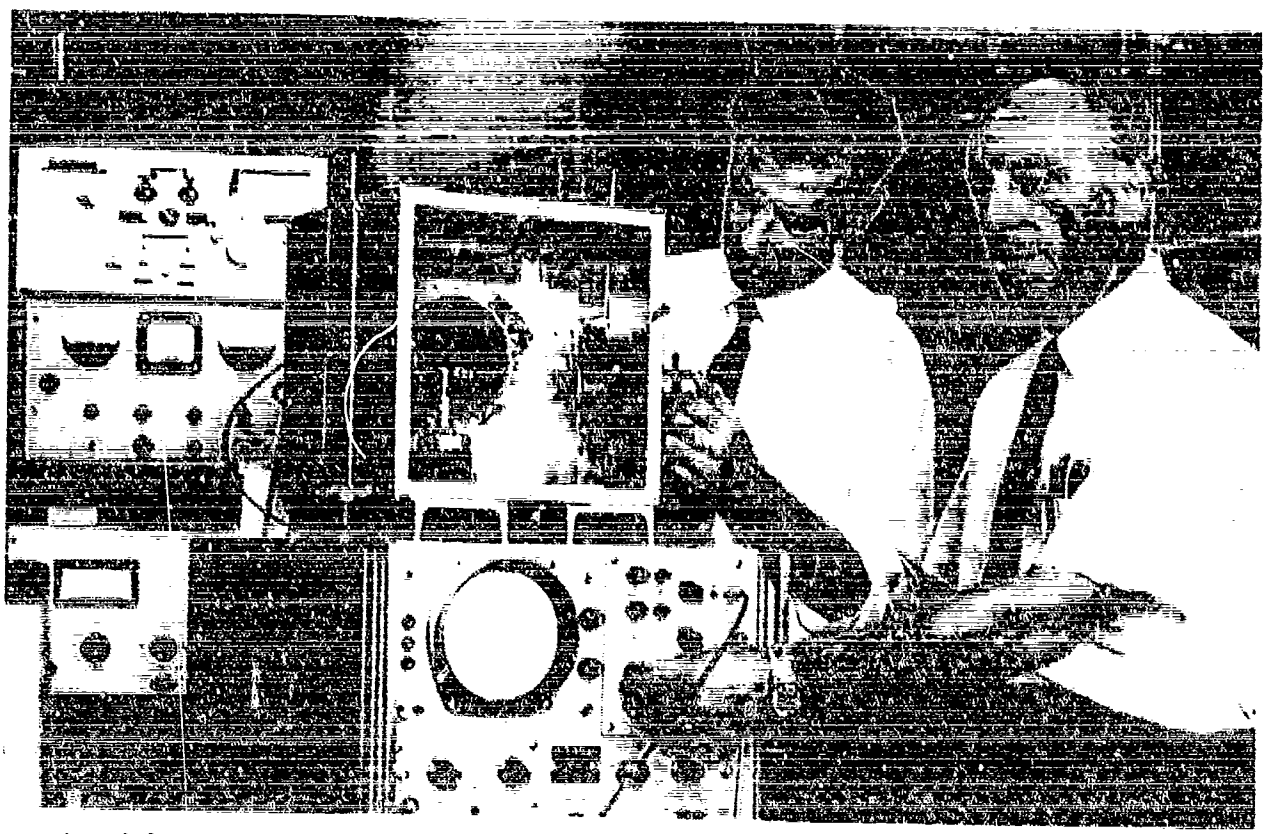

James C. Sethares (left) and Martin R. Stiglitz make adjustments on the apparatus used to obtain displays of resonance patterns.

BALLOON-TRACKING SYSTEM TESTED

AEROSPACE INSTRUMENTATION LABORATORY, AFCRL

A new AFCRL-designed system for locating and tracking research balloons was tested during last August in two balloon flights. The flights originated in Virginia and terminated in New Mexico after a cross-country flight of three days.

Once a balloon is aloft, its path is usually monitored by radar. Obviously, tracking capability is lost if the balloon drifts beyond the range of the radar. The new AFCRL system can locate the balloon anywhere in the continental U.S. The experimental balloon-locating and tracking system takes advantage of the nation's existing VHF Omnidirectional Range (VOR). VOR ground transmitters, operated by the FAA for aircraft navigation, cover the entire U.S. The AFCRL system consists of a conventional VOR receiver, a decoder, and a balloon-borne transmitter which sends the received VOR data on the balloon location back to ground-receiving stations.

The same AFCRL experimental package was carried aboard two different balloons. In a separate experiment for NASA during the same time period, AFCRL launched two balloons from a Wallops Island, Va. site. The NASA balloons carried an earth resources camera system and an airborne recovery system. The NASA flights were terminated over the Atlantic.

These four research balloons were the first to be launched in the East in several years. All four balloons – two AFCRL and two NASA – after an initial ascent which took them out over the Atlantic, reached a maximum altitude of 90,000 feet. At that altitude, the AFCRL balloons were caught in prevailing east winds and transported across the country. The winds took them to New Mexico where the flights were terminated by radio command. When gas was valved from the two NASA balloons, these balloons descended into a prevailing wind system that kept them near the Atlantic Coast.

Francis X. Doherty of AFCRL was project scientist for the AFCRL experiment, and Major Robert M. Brown of AFCRL was in charge of all four balloon launches.

Mr. Francis X. Doherty is a supervisory physicist, and Chief of the Experimental Balloon Activities Branch, Aerospace Instrumentation Laboratory, AFCRL. He is presently engaged in work on high-altitude balloon research and development, and specifically concerned with developing specialized balloon systems for the Air Force and other DoD agencies.

Mr. Doherty attended Boston College, and received his B.S. in Mathematics in 1948 and his M.S. in Physics in 1949. From March 1950 to January 1954, as an oceanographer, he specialized in the study of physical oceanography with the U.S. Naval Hydrographic Office.

Mr. Doherty has several publications on balloons to his credit.

Since late 1967, Major Robert M. Brown has been a project officer at the Experimental Balloon Activities Branch of AFCRL's Aerospace Instrumentation Laboratory.

In June 1957, Major Brown received his B.S. in Naval Science from the U.S. Naval Academy, and in 1963 his B.S. in Electrical Engineering from the University of Michigan through the Air Force Institute of Technology. From 1963 to 1965, he was assigned to the staff of DoD's Manager for Manned Space Flight as an electrical engineer.

Major Brown is the recipient of 21 military decorations for his duties as a fighter pilot in the Air Defense Command (1959-1961) and the Tactical Air Command (1965-1967). He is a member of the I.E.E.E.

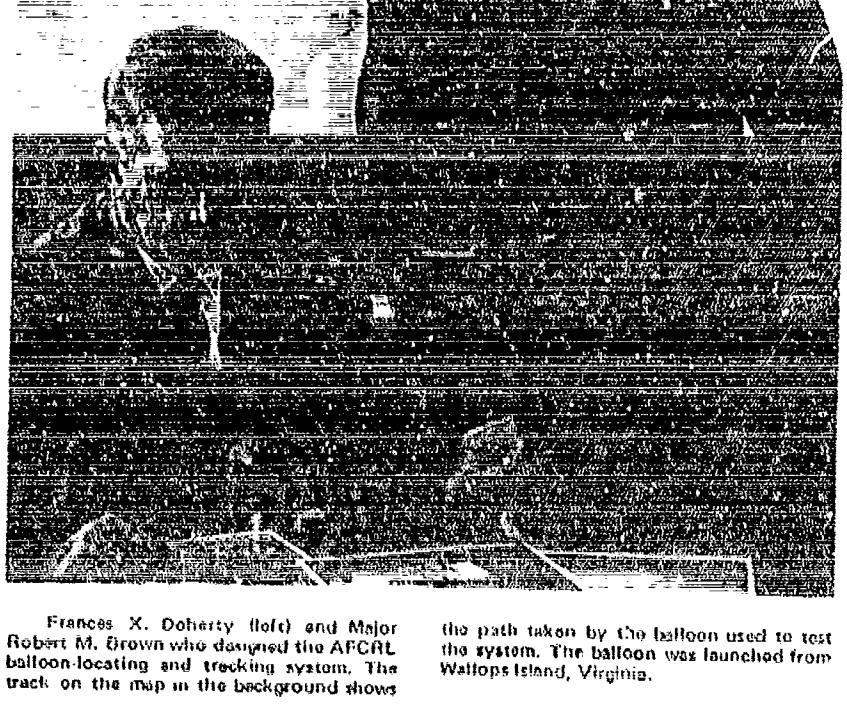

Frances X. Doherty (left) and Major Robert M. Brown who designed the AFCRL balloon-locating and tracking system. The track on the map in the background shows the path taken by the balloon used to test the system. The balloon was launched from Wallops Island, Virginia.

free-molecular flow through a circular tube of finite length

DR. K. S. NAGARAJA, Hypersonic Research Laboratory, ARL

The internal flow of rarefied gases has, in recent years, gained increasing importance due to a variety of space programs. Flights at very high altitudes have increased the need for information pertaining to the low-density regimes, and the flow characteristics in these regions can be obtained only from kinetic theoretic considerations.

The problem of Knudsen or free-molecular flow in tubes of right-circular cross section has relevance to the design of vernier and electric thrustors, to the technology of high-vacuum systems, and to the design and operation of low-density facilities. The free-molecular flow in "infinite tubes" has been considered in many texts on kinetic theory, (e.g., Ref. 1). Kundsen flow in finite tubes has been studied by several authors, and a survey of the available literature is given in Reference 2.

Some recent experiments for determining the flow rates through tubes with openings of 1 to 5 microns in diameter involved tube length to radius ratios of 100 and larger (Ref. 3). When the ratio L/R exceeds 10, the numerical evaluation of the Clausing equation, which gives the flux distribution of molecules along the interior surface of the tube, requires a great deal of computing time even on an IBM 7094. The larger the L/R becomes, the worse the situation gets.

The present work incorporates in the numerical scheme certain properties (indicated in the ensuing discussion) of the flux distribution along the interior surface of the tube. The computing time is not only reduced by this scheme, but the reliability of the data is also ensured. With the flux at the interior surface of the tube thus obtained, the radial flux of molecules at the exist section is calculated by a straightforward integration scheme.

Particles enter a right-circular cylindrical enclosure. The entering flux is assumed to be uniform across the opening section. The neutral-particle mean free path is assumed to be sufficiently large so that the flow remains essentially free-molecular in the tube. Further, it is assumed that the reflection from the wall surface is diffuse.

The arrival rate or flux (at a unit area element) of molecules coming from an area element dS_i located at a distance ℓ_{ij} is given by Ref. 1.

$$d(\dot{n}_j) = \frac{\dot{n}_i}{\pi} \cos\Theta_i \cos\Theta_j \frac{dS_i}{\ell_{ij}^2} \qquad (1)$$

where Θ_i and Θ_j are the angles that the line joining the centers of the area elements makes with the normals to the respective area elements dS_i and dS_j. The quantity $\dot{n}_i$ refers to the flux of molecules at the area element dS_i. Equation (1) is the basic relation in the analysis of the problem.

The radial flux of molecules at the exit section depends on contributions coming from two sources. Some of the molecules entering the tube fly straight to the exit plane. A fraction of the molecules reflected from the wall also contributes to the flux at the exit plane. The flux density $\dot{n}_1$ of molecules entering the tube is known (from the upstream chamber conditions), but the flux of molecules at a point on the interior wall surface is not known a priori. This flux is determined by contributions from molecules entering the tube and those reflected from the wall surface itself. Mathematically, this leads to the following integral equation (called the Clausing equation) for the flux, $\dot{n}_3$, at the interior surface:

$$\dot{n}_3(x, R, L) = \int_0^R \dot{n}_1 H(r,x,R)\, dr + \int_0^L \dot{n}_3(y,R,L)\, I(y,x,R)\, dy. \qquad (2)$$

In equation (2), x refers to the distance of the station (where the flux is to be determined) from the entrance plane, and R and L are the radius and length of the tube, respectively. The functions H and I arise from the use of equation (1) in the analysis, and are therefore geometric in character. Nondimensionalizing the equation by the use of the transformations

$$\bar{n}_3 = \frac{\dot{n}_3}{\dot{n}_1},\quad \bar{x} = \frac{x}{L},\quad \bar{r} = \frac{r}{R} \text{ and } \bar{R} = \frac{R}{L},$$

the Clausing equation can be written as

$$\bar{n}_3(\bar{x}, \bar{R}) = \frac{1}{2\bar{R}}\left[\frac{\bar{x}^2 + 2\bar{R}^2}{(\bar{x}^2 + 4\bar{R}^2)^{1/2}} - \bar{x}\right] + \int_0^1 \bar{n}_3(\bar{y}, \bar{R})\, \bar{I}(\bar{R},\bar{x},\bar{y})\, d\bar{y}. \qquad (3)$$

It can be easily shown that

$$\dot{n}_3(x, R) + \dot{n}_3(1-x, R) = 1 \qquad (4)$$

It, therefore, follows that $\dot{n}_3(x = \frac{1}{2}, R) = \frac{1}{2}$.

The integral equation (3) is solved on an IBM 7094 in the range $0 \leq x \leq \frac{1}{2}$, since the values in the interval $(\frac{1}{2}, 1)$ follow from equation (4). This scheme reduces the computing time considerably. Further, the iteration scheme uses the fact that $\dot{n}_3(\frac{1}{2}, R) = \frac{1}{2}$, and thereby accelerates the computation. This is particularly useful when L/R is 10 or above. The results are also checked against the requirement that the number of molecules entering the tube is equal to the sum of the number of molecules leaving the tube at the exit section and the number of molecules flying straight to the entrance section after experiencing a reflection from the wall surface.

The results of the computations are shown (see also Ref. 4) in Figures 1 and 2 which show, respectively, the flux distribution at the interior wall surface and at the exit plane.

Further work to include intermolecular collisions is being pursued.

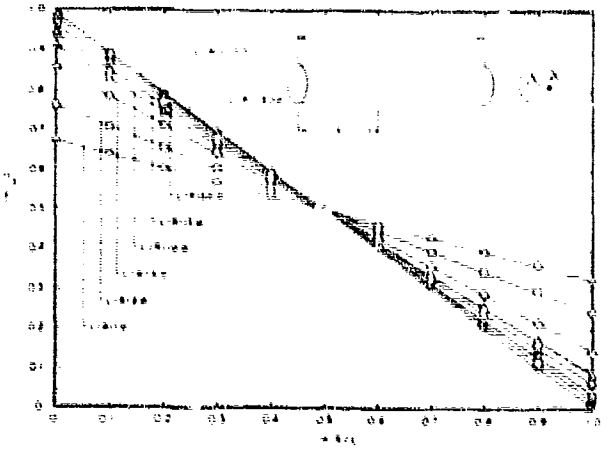

Figure 1. Distribution of the molecular flux density at the wall of the tube.

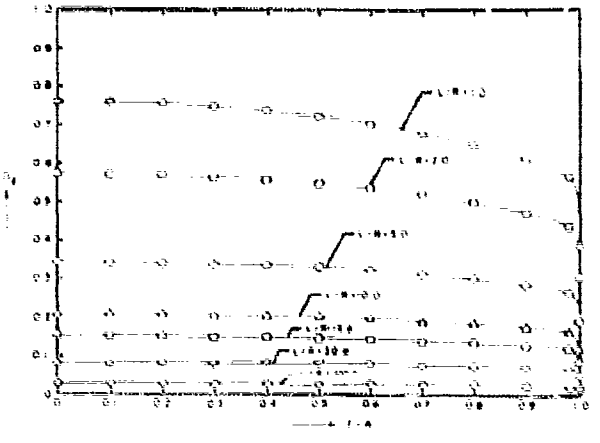

Figure 2. Distribution of molecules in the exit plane.

REFERENCES

(1) Present, R. D., "*Kinetic Theory of Gases*," McGraw-Hill Book Co., Inc., (1958).

(2) Nagaraja, K. S., *A Survey of Some Problems in Rarefied Gas Dynamics*, Vol II, (to be published as an *ARL Report*)

(3) Hedley, W. H. et al, "Flow through Micro-Openings," *First Quarterly Progress Report*, 1 July 1966, Monsanto Research Corporation, Dayton, Ohio.

(4) Nagaraja, K. S., "Free Molecular Flow through a Circular Tube of Finite Length," *ARL 68-0114*, June 1968.

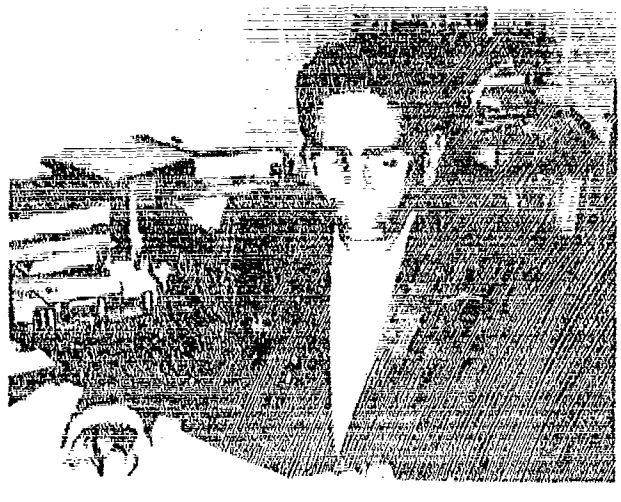

Dr. Kenkanahalli S. Nagaraja is an aeronautical engineer with the Hypersonic Research Laboratory, ARL. He has a B.S. from the University of Mysore, India (1951), an M.S. in Mathematics from Banaras Hindu University, India (1952), and a Ph.D. from Rensselaer Polytechnic Institute (1966).

Dr. Nagaraja has been a research scholar in the Department of Aeronautical Engineering, Indian Institute of Science, Bangalore, India where he studied wing planforms in subsonic and supersonic flight conditions. He has also developed an analysis for obtaining aerodynamic lift distribution on swept wings.

Dr. Nagaraja has been with ARL since September 1962. He is currently doing research in rarefied gas dynamics and V/STOL aerodynamics.

SACRAMENTO PEAK OBSERVATORY, AFCRL

THE VIDEOMETER, A NEW INSTRUMENT FOR SOLAR-FLARE ANALYSIS

Solar flares are the most energetic and complex events on the sun, and induce brilliant and often disruptive events on earth: auroras and magnetic storms. Almost all solar observatories continuously monitor the sun, keeping at least one telescope pointed at the sun throughout the day, and taking pictures of it every few seconds with an automatic camera. Using these photographs, solar astronomers manually and laboriously characterize solar flares by area, peak intensity, and integrated intensity, and assign a class to each.

Paul E. Tallant of AFCRL's Sacramento Peak Observatory in New Mexico has developed instrumentation for classifying solar flares precisely, uniformly, promptly, and in real time. He calls the new instrument for doing this the solar-flare videometer. The videometer promises to become the most important new solar analytical instrument to appear in many years.

Visually, flares, in contrast to benign and fascinating solar phenomenoces, aren't very spectacular. If we look at the sun in the highly filtered light region of hydrogen alpha (Ha), structures on the solar disk are seen in high contrast. In Ha light, a solar flare appears as a sudden, almost instantaneous, bright spot of light which may persist for an hour or so.

The concept of the solar-flare videometer originated with Dr. Richard B. Dunn of the Sacramento Peak Observatory. The basic element is a closed-circuit television system. Sac Peak keeps this TV system trained on the sun continuously. Solar Ha images are presented on monitors located for convenient viewing throughout the Observatory. The videometer takes advantage of signal-processing mechanisms inherent in the [illegible]stem. A line selector is used to obtain a single television line (of the total 525), with the line displayed on an oscilloscope. The video signal along a given scan line is similar to that of a microphotometer scan along a photographic image. With suitable auxiliary processing circuitry, the video signal can be used to measure flare area, peak intensity, and integrated intensity in real time.

The technique, while simple in principle, required many refinements before reaching applicability. First, because flares occur only in active centers characterized by sunspots, sunspot regions are gated off for closer scrutiny. Next, is the plage problem. Plages are extremely bright areas surrounding sunspots. A bright flare must be detected against the bright background of the associated plage area. Amplitude discrimination techniques are used to overcome this problem. Last, flare brightness appears much greater at noon than in the late afternoon because of the viewing angle and the earth's atmosphere. To correct for such diurnal effects, light emitted from a quiet portion of the solar chromosphere is used as a reference. The signal obtained from the chromosphere is used to control the video gain so that the signal level is constant, regardless of the position of the sun.

The videometer permits the astronomer to see the fine structure of flares not apparent in simple photographic analysis. In one case, a flare was visible 16 minutes earlier, and persisted 18 minutes longer than the same flare seen in photographs. The biggest advantage of the videometer is that it eliminates the subjective factor of flare analysis, which presently accounts for the large spread in flare classification by different observers. The videometer, because of the objective and quantitative data that it presents, could lead to a more physically meaningful classification scheme for solar flares.

Mr. Paul E. Tallant is a research physicist at the Sacramento Peak Observatory, New Mexico, where he is presently making flare observations with the videometer, and analysing selected observations. He is also studying the characteristics of the velocity and intensity fields within and beneath calcium plages, the sequence of occurrence of flare-emission points within the calcium supergranule network, and the correlation of CaII H and K intensity with magnetic-field strength.

In 1952, Mr. Tallant received his B.A. in Physics from La Sierra College in Arlington, California. He has taken graduate courses in physics at the University at California, Riverside, California, and is currently engaged in a graduate physics program with the University of New Mexico Extension System at Holloman Air Force Base, New Mexico.

a multipurpose instrument for measuring many properties simultaneously*

DR. W. LEIDENFROST
Professor of
Mechanical Engineering, Purdue University

Much effort is currently being expended to measure and/or calculate the properties of materials over continuously widening ranges of pressure, temperature and, in the case of mixtures, composition. The user of such data is often confronted with different types and quality of information, and many times he must estimate new values for a needed condition. This is true for a single property such as density, viscosity, etc. Even if data can be found, the values usually are not physically concordant.

The present investigation, sponsored by the Air Force Office of Scientific Research, is an attempt to determine simultaneously many properties of substances in order to (a) eliminate sample variations in different tests; (b) secure identical conditions for all different properties; (c) greatly reduce the time and expense otherwise needed for separate measurements. Most of the data is observed absolutely, with high precision over wide ranges of temperature and pressure. This data can then be used for theoretical studies to verify and check models for predicting properties by statistical mechanics, especially for those ranges of temperature where it is impossible to make measurements.

The most significant result of the work done to date has been the design and construction of a unique instrument that can make these property measurements simultaneously. This instrument is shown schematically in Figure 1, and pictorially in Figure 2. It consists of four major parts. A hot body cylindrically shaped with hemispherical ends is enclosed in a similarly formed but slightly larger upper cavity of the cold body which has three parts. The lower part encloses a pressure-measuring device, valves, and a standard platinum-resistance thermometer which is located in the lower spherical cavity formed between the lower and middle parts of the cold body. The upper part suspends and centers the hot body and houses a feed-in device. The system is filled with test fluid either from below or through the feed-in device. The instrument can be sealed off completely for constant volume measurements or, in connection with outside instrumentation, can be used for other types of measurements. The temperature of the instrument is regulated by thermostated fluids channeled bifilarly through passages provided as indicated in Figure 1. The temperature range of the instrument is from -190 degrees C to +650 degrees C; the pressure range extends from vacuum to 500 atmospheres.

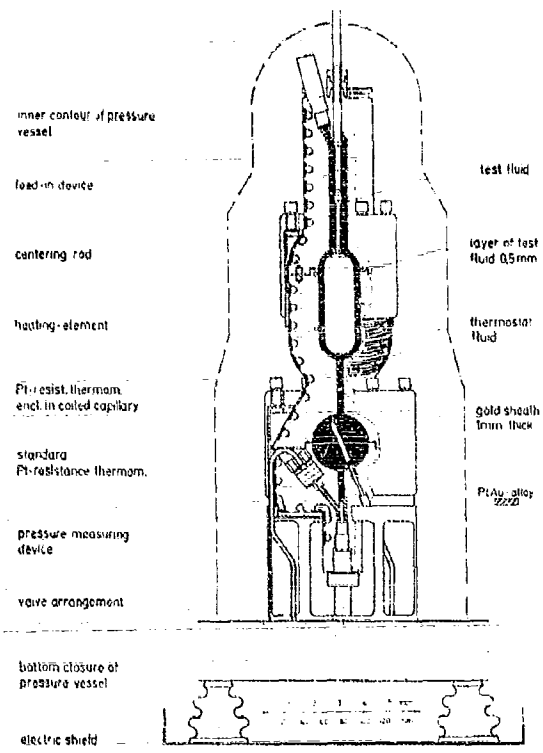

Figure 1. Multipurpose instrument schematic.

Properties which can be determined or measured are as follows:

1. The hot body contains a heater element and serves to generate a thermal potential between it and the cold body when thermal conductivity is to be determined.
2. By establishing an electrical potential difference between the hot and cold bodies, the fluid electrical conductivity can be measured.

(In the first case, Fourier's law is applied. In the second case, Ohm's law is used. The geometric constant for both cases is determined by capacitance measurements.)

Additional properties of fluids can also be determined absolutely under steady-state conditions. These include:

3. Dielectric constant computed from the ratio of capacitance measured with test fluid in the system to that observed under vacuum at the identical temperature.
4. Index of refraction computed from the dielectric-constant values whenever the square-root relationship to the dielectric constant holds true.
5. A.C. electrical conductivity, determined with the aid of a capacitance bridge.

A more detailed description of some of the material of this paper may be found in Reference 1.

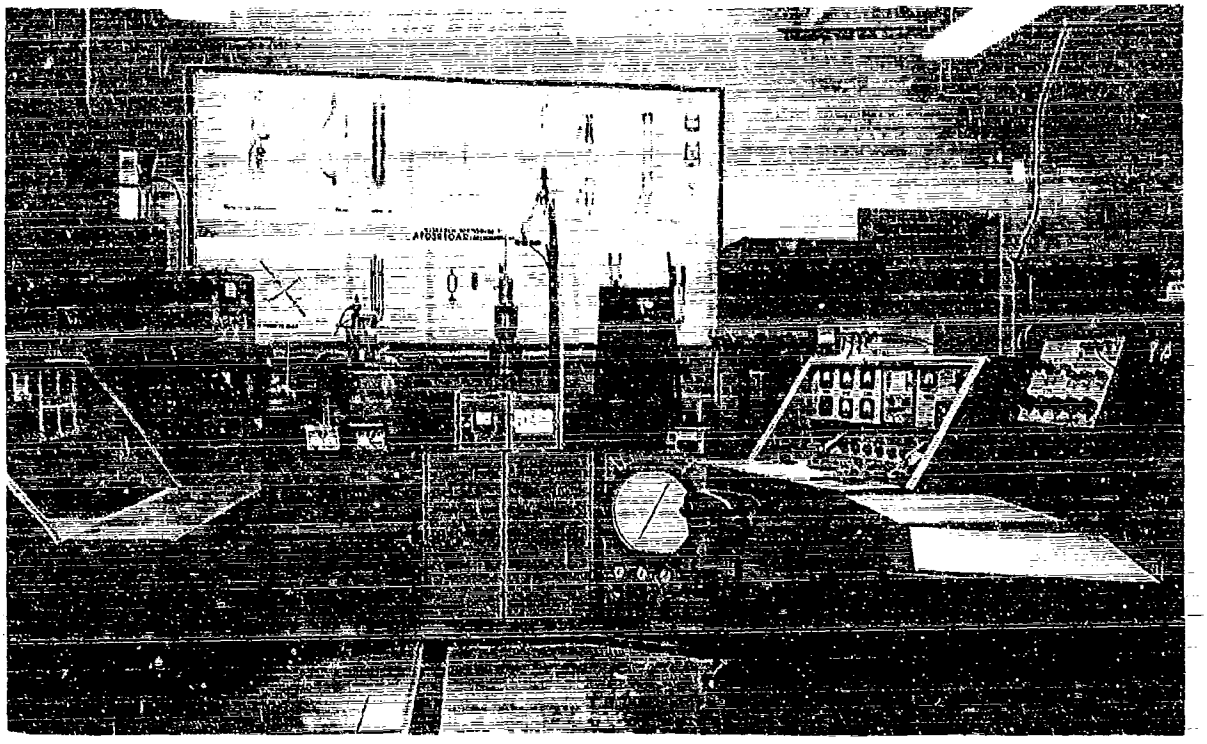

Figure 2. Equipment associated with multipurpose instrument.

6. P-V-T properties of vapor and gases determined by observing the change of pressure with temperature under various constant specific-volume conditions.
7. Specific heats of liquids and solids measured by replacing the heater element with a calorimeter container. Constant heat input by the heater will heat up the sample continuously. The temperature rise with time together with the heat input and the mass of the sample yield the specific heat when there are no heat losses. This is assured by the cold body acting as an adiabatic envelope, its temperature is regulated so as to be identical to the temperature of the container at all times.
8. Vapor pressure of liquids.
9. Compressibility coefficient of liquids.
10. Thermal-expansion coefficient of liquids.
11. Break-down voltage.

In addition to the properties of test fluids listed above, several important properties of the instrument itself can be determined, such as:

12. Thermal expansion coefficient of instrument wall (representing a composite structure). This property is determined by observing the capacitance of the arrangement under vacuum as a function of temperature.
13. Thermal expansion coefficient of centering rod. Measurements are carried out as indicated under 12 above, but with the hot body placed off center in an axial direction.
14. Young's modulus. Pressure change of capacitance with a test fluid (which has a known dielectric constant) is obtained as a function of pressure.
15. The measurements listed under 12 above yield the geometric constant of the arrangement which is equal to the ratio of the area and width of the gap between the hot and cold bodies.

Other possibilities not described in any detail here lead to the following properties determinable absolutely or relatively by the present instrument when operating under unsteady or transient conditions:

16. Diffusivity of heat.
17. Diffusivity of mass.
18. Diffusivity of momentum.
19. Critical-point conditions.
20. Phase-change conditions.
21. Joule-Thomson coefficient.

Note that some of the properties measured are needed to correct other properties observed under perfectly identical conditions. For example, knowing the index of refraction of a test fluid makes it possible to correct thermal-conductivity measurements of the same sample for radiant-heat transfer. Likewise, the observation of the geometric constant as a function of temperature and pressure

makes electrical- and thermal-conductivity values more accurate. Knowing the thermal-expansion coefficient and Young's modulus allows deviations from constant-volume conditions to be corrected when P-V-T data are observed. By measuring many properties simultaneously, it is possible, by cross-checking measurements of related properties, to determine if any observed anomalous variation of one property really exists.

In Figure 2, the capacitance bridge is shown on the right-hand side, next to it are the conductance bridge and the master switch. Further to the left can be seen the potentiometer. The multipurpose instrument itself is mounted on a console shown in the center of the photograph. The mounting platform is electrically insulated from the ground, and is part of the shield of the bridges. The console on the right-hand side of the instrument houses devices for filling and emptying the instrument, and for pressurizing the test fluid. It also contains pressure-measuring equipment. A vacuum pump and thermostats are located on the other side of the instrument. Further to the left is an automatic control unit needed to heat the cold body to the temperature of the calorimeter container when specific heats are measured. Next to the unit is a Mueller bridge used to calibrate the platinum-resistance thermometers built into the cell. The equipment is so arranged that it can be operated by a single observer.

The concept of the multipurpose instrument resulted from property research carried out by the author over the past 20 years with various kinds and types of instruments, many of which he developed himself. (2,3,4) In June 1965, Air Force support was obtained. Although the instrument was designed, developed and built in 1 year, it took almost another full year to line the surfaces wetted by the test fluid with a 1-mm-thick gold layer. By 1968, the laboratory was completed and the instrument became operational. Since then, all necessary calibration has been completed, and property measurements at single conditions of temperature and pressure have been initiated. Some properties were observed over wider ranges of those parameters.

Figure 3 shows the capacitance of the device under vacuum as a function of temperature. The scatter of only a few thousandths of a percent of the measured values around the smooth curve seems to indicate that the wiring, shielding and guarding were done properly.

Figure 4 shows the preliminary results of thermal-conductivity measurements of helium measured along two isotherms in a limited pressure range. Those measurements were the most critical ones because they were used to check out not only the proper functioning of the total system, but also to prove the quality of the gold-bond lining. Improper bonding would cause indeterminable and unrepeatable changes of the geometry of the system. This, in turn, would make it impossible to determine most of the properties listed.

The measured values of the thermal conductivity of helium agree very well with recommended data and seem to confirm a very nonlinear pressure dependence in the low-pressure range.(5) The observation of data at 25°C was carried out rather rapidly. For the 30°C isotherm, more time was allowed for measurements after each pressure change. The data scatter was substantially less, which might indicate that a rather long time is needed to re-establish thermodynamic equilibrium in helium. This point will be

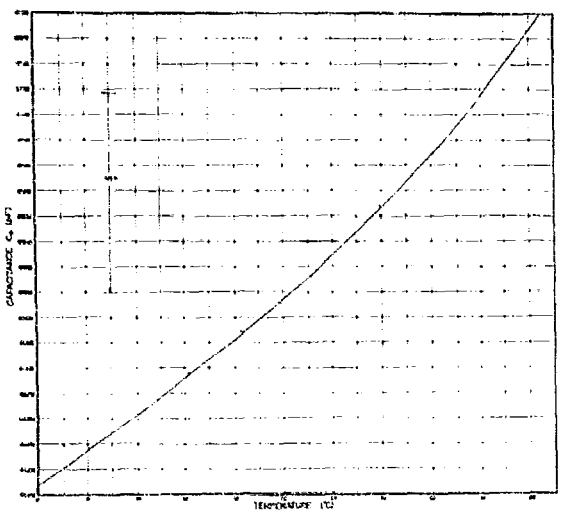

Figure 3. Capacitance of geometrical arrangement under vacuum as a function of temperature.

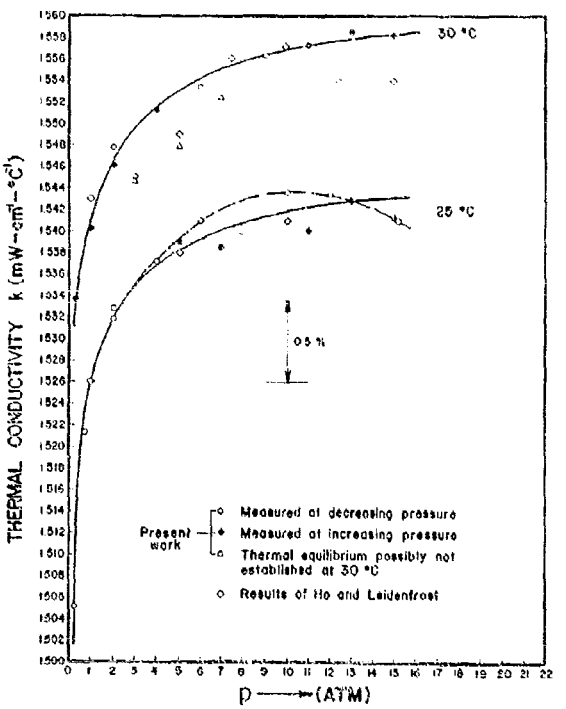

Figure 4. Thermal conductivity of helium gas vs. pressure.

investigated further.

The instrument presently is being used to observe the transport, thermodynamic, and electrical properties of other gases, and will be used in the near future to determine the properties of liquid refrigerants and organic matter. However, many other applications are envisioned for the versatile instrument.

For example, the device is ideally suited for measuring the properties of fluids used as heat-transfer media for cooling electronic components in guidance systems, missile-control and computer devices, high-speed aircraft and space vehicles. These cooling fluids must not only keep the electronic equipment at a safe operating temperature but, in addition, must have the proper electrical properties. They must also be good insulators. And they must meet certain requirements with respect to boiling and freezing, and be chemically inert.

The multipurpose instrument is able to observe all the important properties of these fluids, and so could be used to select the optimum coolant in a minimum time at greatly reduced cost.

REFERENCES

(1) Leidenfrost, W., "Theory and Design Considerations in Developing a Multipurpose Instrument for Determination of Twelve Properties," *Int. J. Heat and Mass Transfer*, (accepted for publication) See also *Proceedings of 6th Conference on Thermal Conductivity*, Dayton, Ohio (1966).

(2) Schmidt, E. and W. Leidenfrost, "Der Einfluss elektrischer Felder auf den Wärmetransport in flüssigen elecktrischen Nichtleitern," *Forschg. Ing. Wes.*, 19, 65-80.

(3) Kestin, J. and W. Leidenfrost, "An Absolute Determination of the Viscosity of Eleven Gases over a Range of Pressure," *Physica*, 25 (1959), 1033-1062.

(4) Schmidt, E.O. and W. Leidenfrost, "Optimierung eines adiabatischen Kalorimeters zur genauen Messung von wahren spezifischen Wärmen schlecht wärmeleitender Substanzen," *Int. J. Heat and Mass Transfer*, 5 (1962), 267-275.

(5) Ho, C.Y. and W. Leidenfrost, "Precise Determination of the Thermal Conductivity of Helium Gas at High Pressures and Moderate Temperatures," *Int. J. of Heat and Mass Transfer*, 1 Monograph (1968), 55-98.

NUCLEAR STUDIES WITH 8-MeV TANDEM ACCELERATOR

WILLIAM A. ANDERSON
General Physics
Research Laboratory, ARL

The Nuclear-Structure Group at ARL is currently engaged in nuclear spectroscopic measurements related to, and defined by, the general problems of nuclear structure. These measurements are accomplished by the detailed investigation of nuclear interactions induced by the charged-particle bombardment of selected target nuclei.

In order to initiate a nuclear interaction by charged-particle bombardment, the incident particle must have sufficient energy to penetrate the Coulomb barrier which exists between the particle and the target nucleus.

The research potential for future nuclear structure studies was considerably enhanced recently with the acquisition, by ARL, of a particle accelerator of unique design and capability. Prior to the installation of this new accelerator, the maximum accelerating energy available to the Group was 2 MeV provided by the standard-charge belt-type electrostatic accelerator of Van de Graaff design. This limited accelerating capability restricted investigations to nuclei at the lower end of the periodic table having an atomic number Z less than about 20. Figure 1 shows a rough comparison of this capability to that of the new tandem accelerator.

This report briefly summarizes the design, operation, and increased capabilities incorporated in this new 8-MeV tandem accelerator and its applications to the wide area of investigations conducted in the ARL Nuclear-Structure Group.

INSULATING CORE TRANSFORMER

The insulating core transformer (ICT) is the source of power for the acceleration system. It is capable of providing 12 milliamperes of current

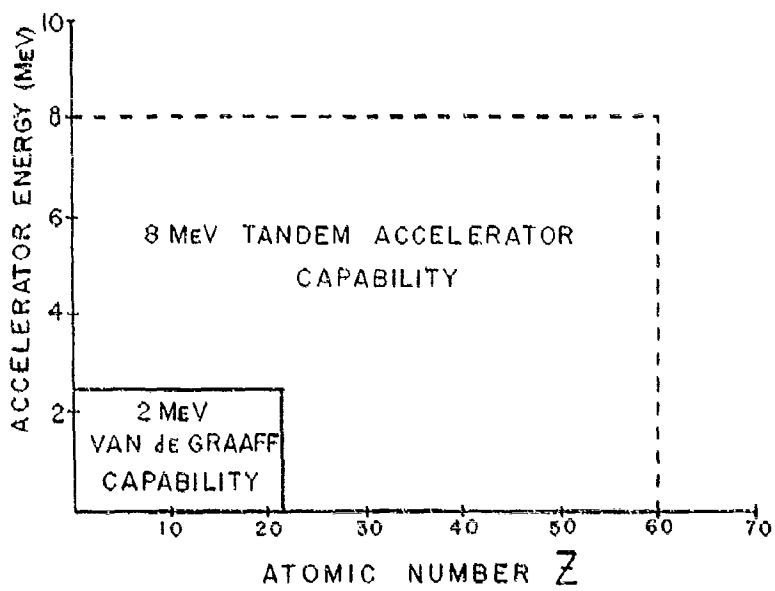

Figure 1. Comparison of the 2-MeV accelerating capability with that of the 8-MeV tandem accelerator.

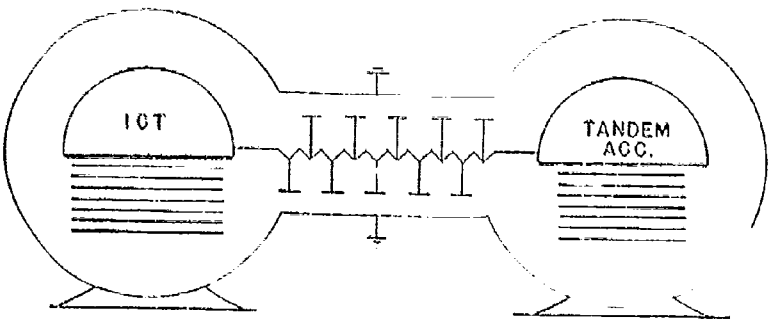

Figure 2. Low-loss RC network.

at a potential of 4 million volts (MV). The 3-phase transformer core, consisting of 3 legs having 44 insulated core segments 15 inches in diameter, produces a magnetic path of high dielectric strength and low reluctance. Each core segment is surrounded by a secondary coil, the output of which is rectified and doubled in a voltage doubler circuit. The doubler circuits are connected in series, and the total voltage obtained is terminated at a highly polished stainless-steel hemisphere at the top of the transformer. Equipotential rings around each triple core section establish a uniform electrostatic gradient along the transformer. Bleeder resistors establish the voltages for the equipotential rings and provide a path for terminal discharge.

The primary power required for operation of the ICT is 60-cycle, 3-phase, and is provided by a servo-controlled variable transformer.

TRANSMISSION LINE

The terminal voltage generated by the ICT is coupled to the acceleration system by a highly efficient, low-loss RC network illustrated in Figure 2.

TANDEM ACCELERATOR

The ion-beam acceleration process is accomplished by two multisection, 8-foot-long acceleration tubes joined together by another highly polished stainless-steel terminal. (Figure 3) This terminal is supported by a very-high-resistance bleeder network similar to the ICT. The electrode-to-electrode voltage gradient for the tubes is established by a voltage divider network and equipotential rings.

In the tandem accelerator, negative ions are accelerated from essentially ground potential to the high voltage terminal, converted to positive ions by an electron stripping process, and further accelerated to ground potential. The ions to be accelerated are originally produced as positive hydrogen ions (H_1^+, H_2^+, and $H_2H_1^+$) obtained from a plasma vessel surrounded by a high RF field. Some negative ions are produced from the initially un-ionized portion by a charge-exchange process with the positive ions in the source.

These negative ions are attracted to the positively charged high-voltage

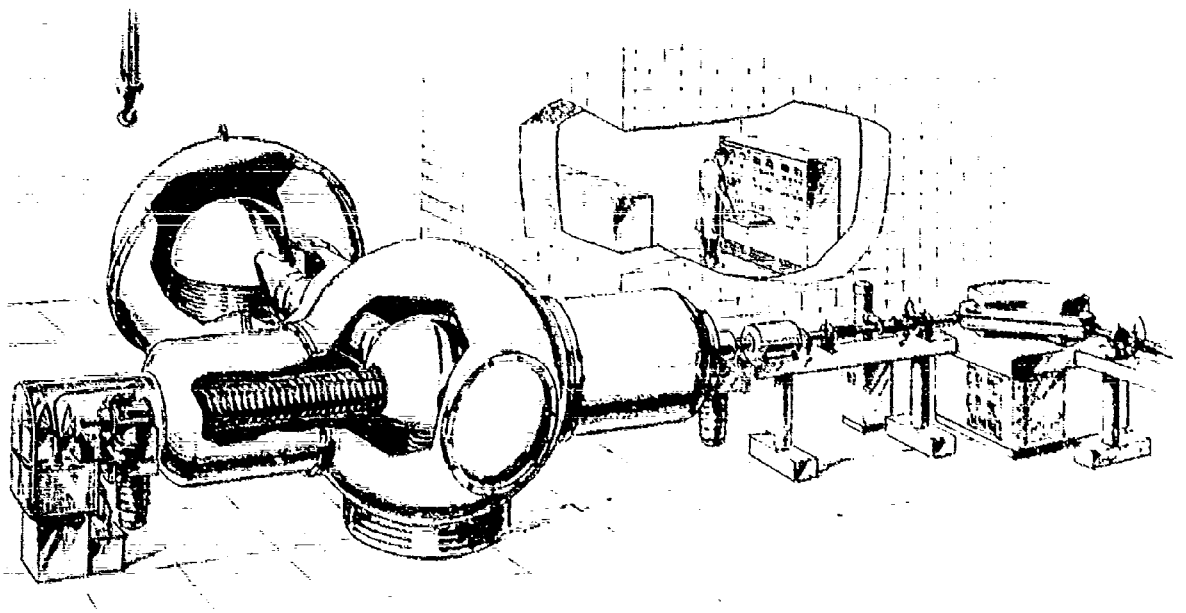

Figure 3. 8-MeV I.C.T. tandem accelerator.

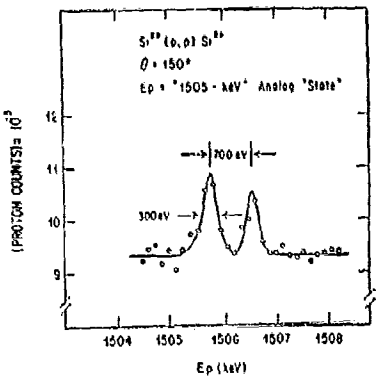

Figure 4. Demonstration of ultrahigh beam-energy resolution capability.

(H.V.) terminal. Upon arrival at the terminal, the ions pass through a stripping canal where the electrons are removed by collision with oxygen-gas molecules. The remaining particles (protons), which already have an energy corresponding to the potential of the H.V. terminal, are repelled away from the terminal toward ground potential, thereby attaining an ultimate energy equal to twice the terminal voltage

With modifications of the ion injector, it will soon be possible to accelerate heavier particles and provide pulsed-beam operation.

ANALYZING MAGNET SYSTEM

The 90° Beam Analyzing System is used to select positive ions of a particular mass, energy and charge. It operates on the principle that a charged particle in motion is deflected by a magnetic field, and that the angle through which the particle is deflected varies with the mass, energy, and charge of the particle. Knowledge of the exact positive ion-beam energy is extremely important for nuclear-interaction experiments. Therefore, the strength of the magnetic field must be accurately determined. This information is provided by nuclear magnetic-flux measurement equipment and a frequency counter.

The deflected, analyzed, positive-ion beam passes through an adjustable slit system placed in the plane of deflection. An error signal is picked up by one edge of the slit if the beam energy changes. This signal is fed back to the ICT power-supply stabilizer for precise terminal-voltage control.

Initial studies with the new ICT tandem accelerator show that it is a powerful new tool for nuclear-structure research. Beam-energy resolution of about ± 200 eV or better has been demonstrated on many occasions. (See Figure 4) It is believed to be the largest ultrahigh-resolution accelerator presently in existence.

The nature of the research program which requires such a sophisticated tool involves the continued development of a systematic study of energy levels of low-medium mass nuclei. The nuclear reactions produced by the accelerator beam, when spectroscopically analyzed, provide data on properties of energy levels. The comparison of these data is made with theoretical predictions to determine the nuclear structure, nuclear interactions, and validity of various theoretical nuclear models.

Mr. William A. Anderson is chief technician in charge of accelerator operations in the Nuclear Branch, General Physics Research Laboratory, ARL.

In March 1959, he enlisted in the USAF and was an honor graduate from the Electronics Tech. School. He was subsequently assigned to the Strategic Air Command as a communication and navigation technician at March AFB, California. During a three-year tour there, he attended U.S.C., Los Angeles in his off-duty hours. In August 1962, he was assigned to ARL, and honorably discharged in December of the same year.

Mr. Anderson joined ARL as a civilian in January 1963. He attends classes at Wright State University, and will soon receive his B. S. in Physics. He is a coauthor of a paper presented at a meeting of the American Physical Society 27-30 April 1964.

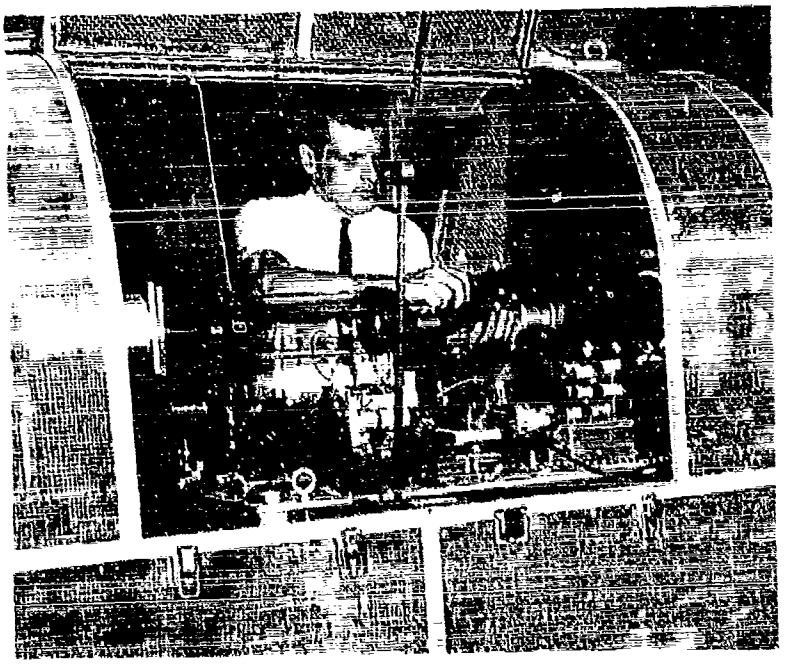

Mr. W. A. Anderson adjusting the ion-source section of the new 8-MeV tandem accelerator.

gravity-gradient-stabilizing torques

MAJOR JAMES C. MC SHERRY
Det. 6 (LOOAR) OAR

The technique of stabilizing satellites by exploiting the torques generated by differences in the spacecraft moments of inertia is known as gravity-gradient stabilization. The technique is quite simple. By designing a satellite to have large differences between the moments of inertia about the spacecraft axes, the satellite, with appropriate damping, will stabilize about the local vertical.* The best example of a gravity-gradient-stabilized satellite is the moon. The slight differences in the moments of inertia of the moon create small torques which, over the years, have stabilized the moon such that one side always points to the earth.

Artificial earth satellites, such as OAR's OV1, use this technique for stabilization when experiments require the spacecraft to view the earth. The usual technique is to extend very long slender rods with small tip masses to create the favorable inertia ratios. On the OV1 satellite, there are 5 booms. Two are essentially vertical and are 62 feet long; the other 3 are horizontal and 50 feet long. Other satellites have used 1 to 6 booms, and lengths have been from 30 feet to 750 feet. Damping mechanisms vary widely, but usually rely on interaction with the earth's magnetic field or relative motion between booms to dissipate energy. But, to fully appreciate these mechanisms, one must first understand the basic concept of gravity-gradient stabilization: the generation of the stabilizing torques. In other words, how can you expect a satellite to stabilize simply by sticking out a long rod?

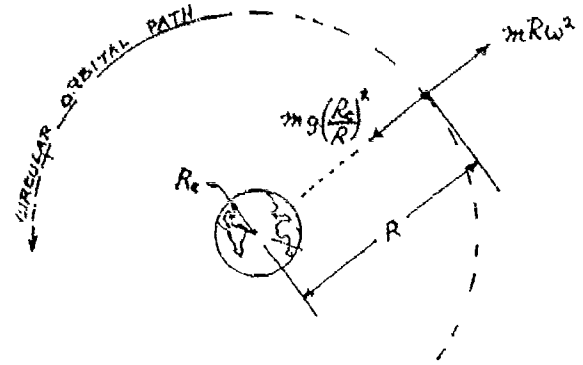

Figure 1. Satellite balanced between centrifugal and gravitational forces.

THE FORCES

To best explain the mechanism which produces the stabilizing torque, we should return to the basic concept of circular orbits. That is, the satellite is precisely balanced between centrifugal and gravitational forces, as in Figure 1.

Local vertical—a line from a point in space to the center of the earth.

The gravitational force is $mg\left(\frac{Re}{R}\right)^2$ and always acts towards the center of the earth. The centrifugal force is $mR\omega^2$, where ω is the orbital angular velocity, expressed in radians per second. Expressed in vector notation, it is $m\vec{\omega} \times (\vec{r} \times \vec{\omega})$; thus its line of action is parallel to the orbital plane.

TORQUE GENERATION IN THE PITCH PLANE

Imagine a satellite made up of two equal masses separated by a very long weightless rod, as sketched in Figure 2a. The gravity-force action on mass 1 is smaller

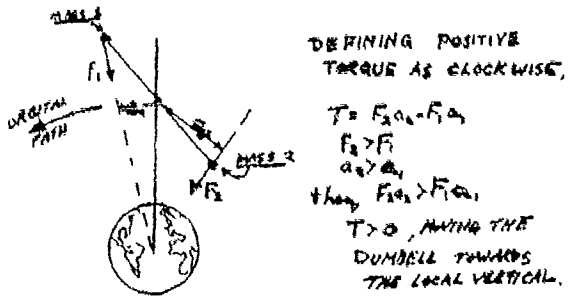

Figure 2a. Pitch plane. Gravitational torque imbalance.

than the force acting on mass 2. The moment arm through which the force acts is shorter for mass 1 than for mass 2. Therefore, the net gravitational torque will rotate the dumbbell towards the local vertical. The centrifugal torques exactly cancel because the stronger force has the shorter arm, and vice versa. (Figure 2b contains a derivation of this cancellation.)

TORQUE GENERATION IN THE ROLL PLANE

The centrifugal forces acting on mass 1 and mass 2 have equal arms. Therefore, the force imbalance generates a clockwise torque in this view. The gravitational force on mass 2 is less than on mass 1, and has a shorter arm. The resulting torque will also be clockwise. Therefore, both centrifugal and gravitational forces produce a restoring torque to move the dumbbell into the orbital plane.

TORQUE GENERATION IN YAW

For visualization of the yaw torque, imagine that our dumbbell satellite is stabilized along the local vertical, and that another mass and boom combination has been added

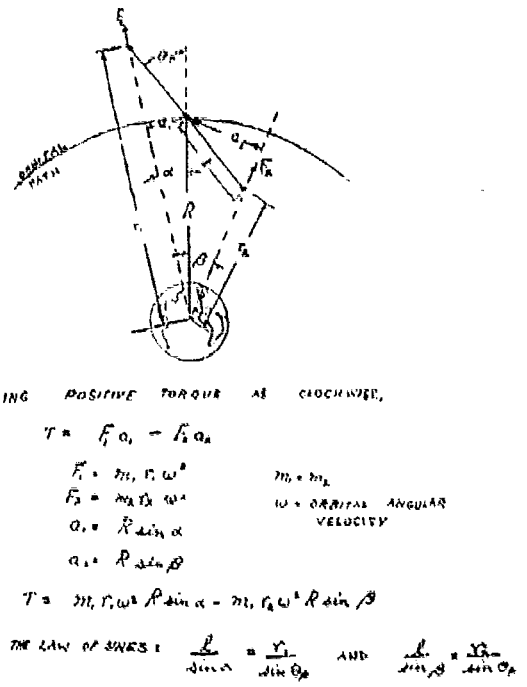

Figure 2b. Pitch plane. Centrifugal torques balance.

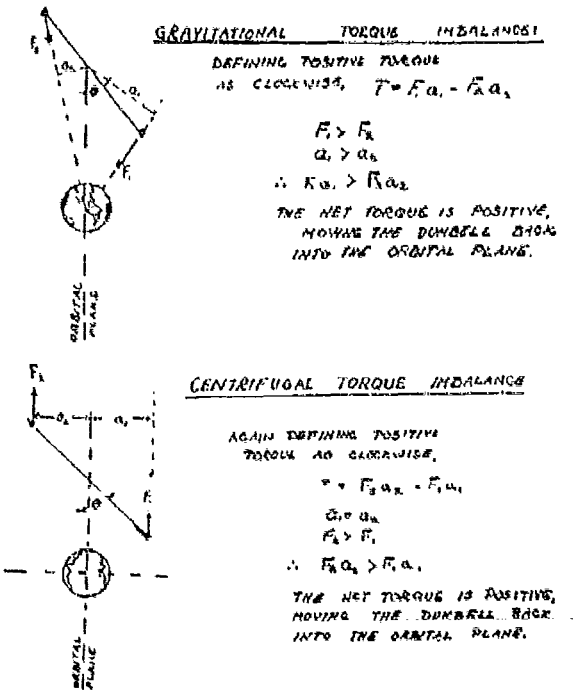

Figure 3. Torque generation in the roll plane.

normal to the first boom. The angle between this boom and the velocity vector is Θ_y. Note that no gravitational torque exists on this horizontal boom. The centrifugal forces are equal for each mass, but a small angle exists between them. The forces can be considered as the resultant of a vertical and horizontal component. The vertical components exert no torque, but the horizontal components are equal and opposite, resulting in a couple which rotates the satellite to align the second boom with the velocity vector.

DAMPING

It is obvious that the torques generated by the imbalance of the centrifugal and gravitational forces depend on the angle by which the boom is offset from the local vertical and the velocity vector. If no damping is present, the satellite would oscillate like a perfect pendulum from its original offset to a position equally offset on the other side of the reference line. Therefore, for true stabilization, some sort of damping mechanism is essential to the gravity stabilization of a satellite.

RELATIVE SIZES OF THE TORQUES

From the above analysis, it is apparent that the strongest torque is in roll, where both gravitational and centrifugal forces contribute to the restoring torque. The second strongest would be in pitch where gravity alone generates the torque. The weakest is in yaw, where only a small component of the centrifugal force is contributing to the torque.

The equations for the torques produced bear out this relationship. Ignoring second-order effects (which are usually considered), the equations are:

$$T_{Roll} = 4/2\,(I_{Pitch} - I_{Yaw})\,\omega_0^2 \sin 2\theta_{Roll}$$

$$T_{Pitch} = 3/2\,(I_{Roll} - I_{Yaw})\,\omega_0^2 \sin 2\theta_{Pitch}$$

$$T_{Yaw} = 1/2\,(I_{Pitch} - I_{Roll})\,\omega_0^2 \sin 2\theta_{Yaw}$$

where I is the satellite moment of inertia about the respective axis, ω_0 is the satellite's orbital angular velocity, and Θ is the angular offset from the desired position. These equations were first derived by Lagrange some 200 years ago during his work on librations of the moon.

Examination of the equations shows that a satellite in circular orbit with dissimilar moments of inertia will eventually be stabilized with its minimum moment of inertia (yaw) aligned with the local vertical, and its maximum moment of inertia aligned with its instantaneous velocity vector.

As can be imagined, these torques are exceptionally

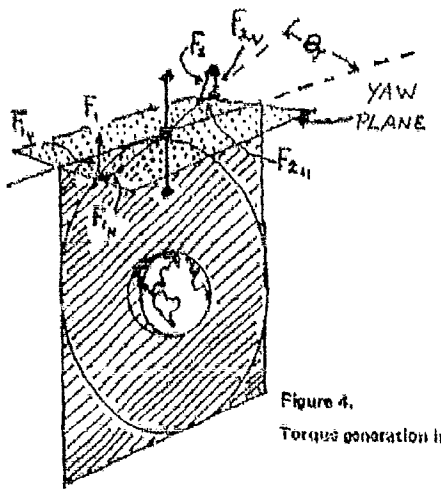

Figure 4.
Torque generation in the yaw plane.

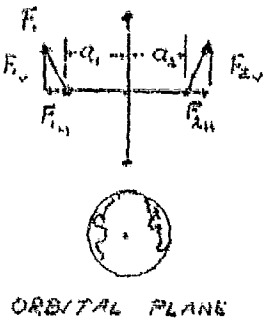

NOTE: NO TORQUE

$T = F_{2_V} a_2 - F_{1_V} a_1$

$a_1 = a_2$

$F_{2_V} = F_{1_V}$

$\therefore T = 0$

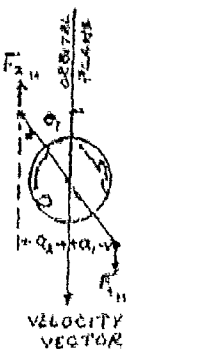

$T = F_1 a_1 + F_2 a_2$

then $T > 0$

MOVING THE DUMBELL BACK TOWARDS THE VELOCITY VECTOR

small. For example, on OV1-17, if the vehicle is displaced to 5° off the desired yaw direction, the restoring torque is only 0.0000022 foot-pound. However, in the weightless environment of circular orbit, the disturbances are also quite small, and this seemingly infinitesimal torque is sufficient.

SUMMARY

Gravity-stabilized satellites are possible because of small differences in the delicate balance between gravitational and centrifugal forces in a circular orbit. If a satellite is properly designed to use the torques generated by these slight differences, an earth-oriented satellite can be manufactured that will require no continuous power for its stabilization.

HIGH-TEMPERATURE SEMICONDUCTOR

DR. ROBERT H. REDIKER, Department of Electrical Engineering and Center for Materials Science and Engineering, M.I.T.

Since the early 1950s, the Air Force has been very interested in the development of semiconductor components that will operate effectively at higher temperatures than available devices. Examples of Air Force-sponsored programs to extend the high-temperature limit of semiconductor devices are those that led to the development of silicon transistors which operate at temperatures up to a limit of 200°C, those programs to develop gallium-arsenide transistors, and those to develop components of silicon carbide.

In response to this continuing need, the Air Force Office of Scientific Research is sponsoring basic research by Professor R. H. Rediker at M.I.T. on the conduction mechanisms and technology of single-crystal stannic oxide, SnO_2. Since SnO_2 is physically and chemically stable at elevated temperatures, and is a wide-bandgap semiconductor with a bandgap of 3.7 electron volts, it seems suitable for semiconductor components which could operate at temperatures up to 500°C.

While single crystals of SnO_2 have previously been obtained in the laboratory by several different techniques, (1-6) the vapor-phase growth technique, which is described below, is more comparable to that used by Schaffer (7) to grow Al_2O_3 in that no carrier gases are used and all reactions and growths occur at low pressure. The crystals are grown from the vapor at 1250°C and at 10 torr pressure using the reaction

$$SnCl_4 + 2H_2 + O_2 \rightarrow SnO_2 + 4\,HCl\,.$$

The stannic chloride ($SnCl_4$) is obtained from the reaction of tin and chlorine gas at 100°C and 10 torr pressure

$$Sn + 2Cl_2 \rightarrow SnCl_4\,.$$

The resistivity of the tin-oxide semi-

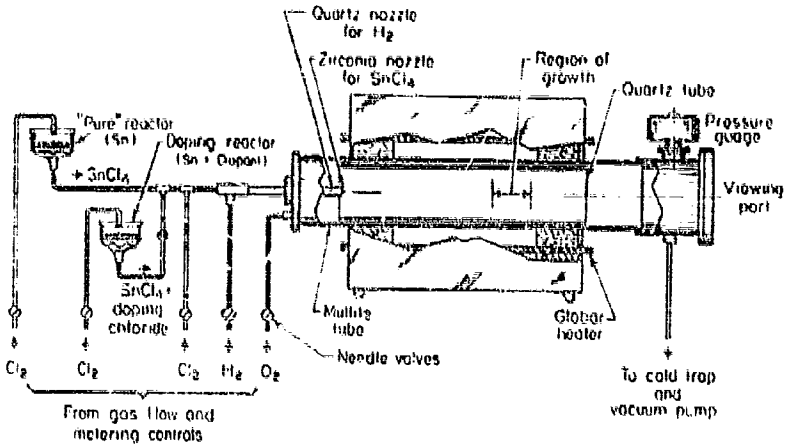

Figure 1. Stannic-oxide crystal-growing system. The drawing is not to scale; the actual mullite tube is 90 cm long, 5 cm i.d.

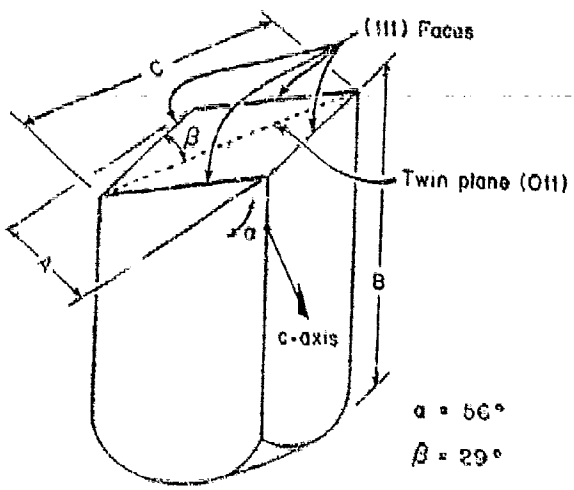

Figure 2. Stannic-oxide crystals: (top) artist's sketch of a crystal illustrating growth habit; and (bottom) photograph of two typical crystals.

conductor is controlled by adding selected impurities such as antimony to the tin charge.

The crystal-growing apparatus is shown in Figure 1. Note that by adjusting the relative amount of chlorine flow through the "pure" reactor, which contains only tin, and through the doping reactor, the resistivity of the tin oxide grown can be predetermined; also, by varying this relative amount during a run, a desired resistivity profile can be obtained. This and other features of the system have been described more thoroughly in a recent publication in the *Journal of the Electrochemical Society*. (8)

A photograph of two typical crystals that have been grown is shown in Figure 2. Spectrochemical analyses of such crystals indicate that they are purer than any previously reported. Electrical measurements have yielded a value for the Hall mobility at 77°K of 1200 cm^2/volt sec, which is higher than any previously reported and is consistent with the higher purity. The electrical properties of a crystal doped with antimony to a room-temperature resistivity of 0.1 ohm-cm n-type are shown as a function of temperature in Figure 3. Plotted are the Hall mobility μ, the resistivity ρ, and the conduction electron concentration n determined from the equation, $n = 1/e\mu\rho$, where e is the electronic charge. The electrical characteristics in Figure 3 indicate that single-crystal SnO_2 should be usable in semiconductor components which operate at temperatures of 500°C; but much more basic research on the conduction mechanism and technology are still required before practical SnO_2 high-temperature components can be built.

REFERENCES

(1) Morgan, D. F. and D. A. Wright, "Electrical Properties of Single Crystals of Antimony-Doped Stannic Acid," *Brit. J. Appl. Phys.*, 17 (1966), 337.

(2) Kunkle, H. F. and E. E. Kohnke, "Flux Growth of Stannic-Oxide Crystals," *J. Appl. Phys.*, 36 (1965), 1489.

(3) Marley, J. A. and T. C. MacAvoy, "Growth of Stannic-Oxide Crystals from the Vapor Phase," *J. Appl. Phys.*, 32 (1961), 2504.

(4) Reed, T. B., J. T. Roddy and A. N. Mariano, "Vapor Growth of Tin-Oxide

Crystals," *J. Appl. Phys.*, 33 (1962), 1014.

(5) vanDaal, H. J., "Polar Optical-Mode Scattering of Electrons in SnO_2," *Solid State Comm.*, 6 (1968), 5.

(6) Nagasawa, M., S. Shionoya and S. Makishima, "Vapor-Reaction Growth of SnO_2 Single Crystals and their Properties," *Japan. J. Appl. Phys.*, 4 (1965), 195.

(7) Schaffer, P. S., "Vapor-Phase Growth of Alpha Alumina Single Crystals," *J. Amer. Ceram. Soc.*, 48 (1965), 508.

(8) Fonstad, C. G., A. Linz and R. H. Rediker, "Vapor-Phase Growth of Stannic-Oxide Single Crystals," to be published in the *J. Electrochem. Soc.* (1969).

Dr. Robert H. Rediker, Professor of Electrical Engineering at M.I.T., received his S.B. in Electrical Engineering (1947) and his Ph.D. in Physics (1950), both from M.I.T. He was associated with the M.I.T. Lincoln Laboratory for 14 years, and headed the Applied Solid-State Physics Group from 1959-1966. Since 1966 he has been on the faculty at M.I.T. where his current interests include opto-electronic semiconductor devices and high-temperature semiconductor devices.

Dr. Rediker is the author of more than 50 professional articles, is a Fellow of both the Institute of Electrical and Electronics Engineers and the American Physical Society, and is the recipient of the 1969 David Sarnoff Award of the IEEE. His research on the physics of semiconductor luminescence and high-temperature semiconductors is sponsored by the Solid State Sciences Division, Directorate of Physical Sciences, AFOSR.

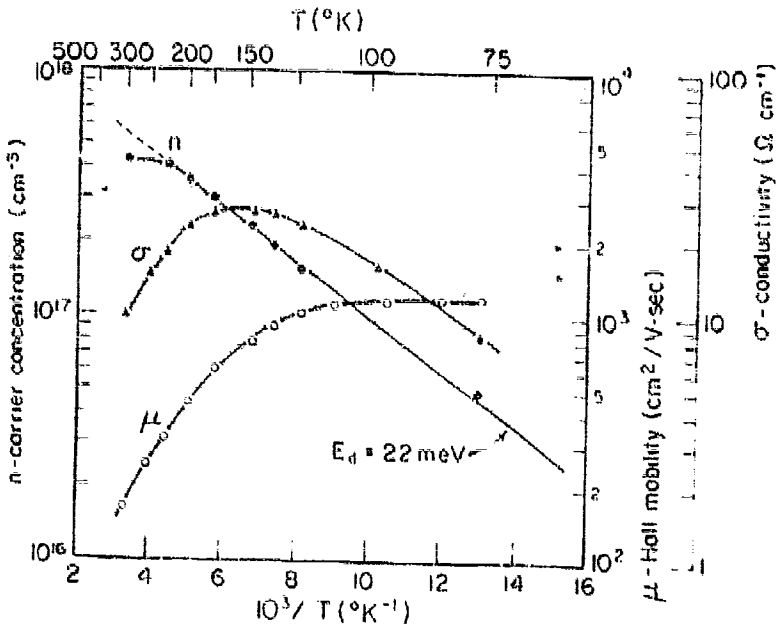

Figure 3. The Hall mobility, resistivity, and conduction electron concentration of an antimony-doped SnO_2 sample measured for temperatures between 77°K and 300°K.

Dr. Rediker (left) is shown here adjusting the controls on the crystal-growing apparatus with one of his graduate students, Cliff Fonstad

numerical optimization techniques

DR. ANGELO MIELE
Department of Mechanical and Aerospace Engineering and Materials Sciences, Rice University; and
LT COL PAUL J. DAILY
Directorate of Mathematical Sciences, AFOSR

For several years Professor Angelo Miele of Rice University, under a grant from the Applied Mathematics Division, AFOSR, has been conducting research on aerodynamic configurations optimum for flight in the supersonic, hypersonic, and free-molecular flow regimes. The methods of the calculus of variations in one or two independent variables have been employed in order to determine configurations having minimum drag, minimum ballistic factor, or maximum lift-to-drag ratio.

During these research activities, Professor Miele identified a need for concentrated research to develop new and improved numerical techniques applicable to problems arising in aerospace applications, such as optimal flight trajectories and optimal aerodynamic shapes. Typical areas of mathematical investigation include first-variation methods, second-variation methods, and two-point boundary-value problems. In two recent reports, Professor Miele discloses significant accomplishments related to the restoration of constraints in holonomic problems, and to gradient methods in mathematical programming. (1,2)

In problems described by holonomic equations (equations which may be algebraic or transcendental), a nominal state approximating a solution (but not satisfying all the

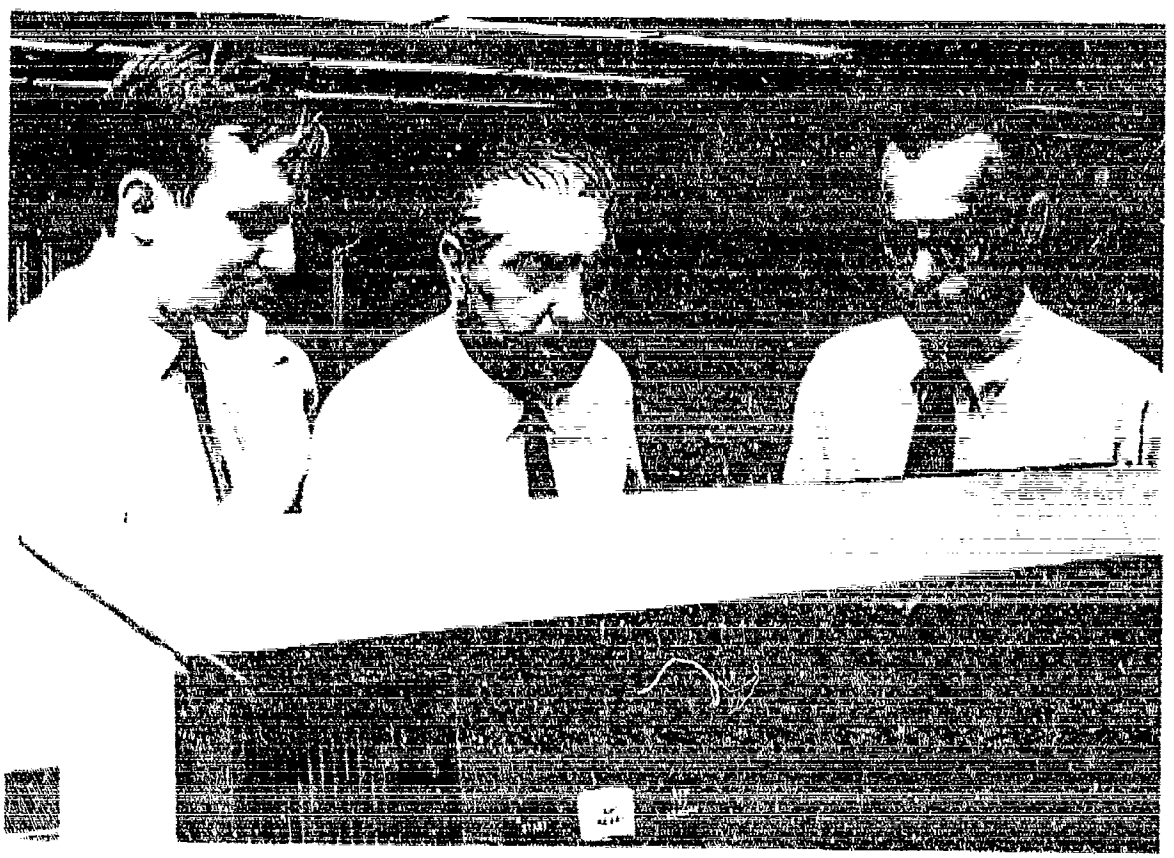

From left: E. E. Cragg, Prof. A. Miele (center) and J. C. Heideman taxing the computer with numerical optimization problems. Mr. Cragg and Mr. Heideman are graduate students in Aero-Astronautics.

equations exactly) may be available. Starting from the nominal state, one may wish to determine a varied state, close to the nominal state and satisfying all the equations more exactly. This situation arises in some of the iterative algorithms for minimizing functions of variables subject to holonomic constraints, namely, first-variation and second-variation methods.

Professor Miele has developed a systematic procedure to change the state in an optimal way: this is the requirement that the constraints be restored with the least-square change of the coordinates. A resulting algorithm has been applied to several numerical examples based on systems described by p algebraic or transcendental equations involving n variables, with n greater than p. It is assumed that a nominal state, not satisfying all the equations, is given. Using a Burroughs B-5500 computer and double precision arithmetic, an iterative procedure is applied leading to a varied state satisfying all of the equations to a desired degree of accuracy based upon a preestablished performance index.

While considering the problem of minimizing a scalar function f(x) of an n-vector, x, Professor Miele reviewed the ordinary gradient algorithm and the Fletcher-Reeves algorithm. Compared with the ordinary gradient method, the Fletcher-Reeves algorithm has the advantage of high speed since it produces quadratic convergence. Compared with other conjugate gradient methods (such as the Davidon variable-metric algorithm), it has the advantage of simplicity of concept and small storage requirement while yielding comparable computing time. A new accelerated gradient method, the memory gradient method, for finding the minimum of a function f(x) whose variables are unconstrained has recently been reported by Professor Miele. The new algorithm can be stated as follows:

$$\tilde{x} = x + \delta x, \qquad \delta x = -\alpha g(x) + \beta \delta x'$$

where δx is the change in the position vector x, $g(x)$ is the gradient of the function f(x), and α and β are scalars chosen at each step so as to yield the greatest decrease in the function. The symbol $\delta x'$ denotes the change in the position vector for the iteration preceeding that under consideration.

This algorithm, for a quadratic function, reduces to the Fletcher-Reeves algorithm; thus, quadratic convergence is assured. However, for a nonquadratic function, initial convergence of this method is faster than that of the Fletcher-Reeves method because of the extra degree of freedom available. A two-dimensional search is required at each iteration as opposed to the one-dimensional search of the Fletcher-Reeves algorithm because of this added degree of freedom; however, for a test problem, the number of iterations was about 40-50% that of the Fletcher-Reeves method, and the computing time about 60-75% that of the Fletcher-Reeves method, using comparable search techniques.

A continued investigation combining the memory gradient and restoration of constraints techniques has been conducted by Professor Miele. The preliminary results should be available in report form in the near future.

REFERENCES

(1) Miele, A. and J. C. Heideman, "The Restoration of Constraints in Holonomic Problems," *Aero-Astronautics Report No. 39*, Rice University (1968).

(2) Miele, A. and J. W. Cantrell, "Gradient Methods in Mathematical Programming–Part 2 - Memory Gradient Method," *Aero-Astronautics Report No. 56*, Rice University (1969).

Dr. Angelo Miele has been a Professor of Astronautics at Rice University, Texas since 1964. Prior to that, he was a Research Assistant Professor of Aeronautical Engineering at the Polytechnic Institute of Brooklyn (1952-1955); a Professor of Aeronautical Engineering at Purdue University (1955-1959); and a Visiting Professor of Aeronautics and Astronautics at the University of Washington (1961-1964). He has also acted as a consultant to the Guided Missiles Division of the Douglas Aircraft Co., and the Allison Division of the General Motors Corp., and has been associated with the Boeing Scientific Research Laboratories as Director of Astrodynamics and Flight Mechanics (1959-1964).

Dr. Miele has a Doctor's degree in Civil Engineering (1944), and a Doctor's degree in Aeronautical Engineering (1946), both from the University of Rome, Italy. He has authored or coauthored more than 100 technical papers in his field. He is an Associate Fellow of the American Institute of Aeronautics and Astronautics, a Senior Member of the American Astronautical Society, and a Member of the Associazione Italiana di Aerotecnica, Associazione Italiana Razzi, and Sigma Gamma Tau. Dr. Miele is also an Associate Editor of the Journal of the Astronautical Sciences and Editor-in-Chief of the Journal of Optimization Theory and Applications. He was recently elected a Corresponding Member of the International Academy of Astronautics.

MEASUREMENT OF UPPER-AIR POLLUTION

OPTICAL PHYSICS LABORATORY, AFCRL

Air pollution is worsening. So everybody says. But is it? And if it is, at what rate? Have increased pollutants from automobile exhausts merely balanced the amount of pollutants generated a half century ago by the wood and soft coal heating of individual homes?

All this is by way of saying that we really don't have any way of gauging long-term trends. In this connection, the concentrations of pollutants–or aerosols–found at altitudes between about 7 and 35 km may prove instructive. Aerosols at these altitudes have less day-to-day variability and may provide a better way of measuring long-term trends than measurements of air pollutants nearer the surface. (In addition to man's contributions to upper-air pollutants, aerosols in the upper atmosphere have come from a variety of other sources–volcanic eruptions, meteoric dust, and dust from the tropics carried aloft by convective currents.) The Air Force is not interested in air pollution as such, but is interested in the extent to which pollutants mask the data obtained from IR and visual sensors aboard aircraft and satellites. It is this problem that gives rise to AFCRL's interest in the field.

In recent years, a number of researchers concerned with atmospheric aerosols have begun to use lasers to probe the atmosphere for aerosol concentrations at various altitudes. With this technique, a laser beam is projected upward and measurements are made of the amount of light scattered by aerosols and molecules at given altitudes. Most of the researchers entering this new field have evolved their own measurement procedures independently. Lack of uniformity in measurement procedures makes it difficult to correlate the results obtained by different observers.

At the Second Conference on Laser Atmospheric Probing held last April 15-16 at the Brookhaven National Laboratories, Louis Elterman of AFCRL, a pioneer in the measurement of aerosol concentrations by light-scattering techniques, reviewed six areas where standardization is important. He has suggested that the establishment of uniform standards can be based on the following six considerations:

1. Atmospheric conditions vary, causing variations in the optical transmission of the laser path. This can affect the results of measurements. Researchers to date have ignored the problem or have assumed the transmission of the path to be constant. Elterman suggests that it should be treated as a variable.

2. The choice by researchers of a normalizing altitude to be used for calibration appears in many instances to be arbitrary. The choice should be based on the best current knowledge of the distribution of atmospheric constituents. The same normalizing altitude should be used by those with the same or similar measurement objectives.

3. Altitude resolution is a problem in probing the atmosphere because laser probers use considerably differing altitude intervals from which the laser pulse return is measured. Comparison of results among laser probers can be more meaningful if some standards for altitude resolution are established.

4. and 5. Elterman treats molecular measurements and aerosol measurements as separate entities; but his recommendations in these areas are combined here. Contained in the total scattering response, we have scattering from both atmospheric molecules and from aerosols. Not only is it desirable to separate the relative amounts of scattering from each, but one would also like to know the absolute values of aerosol parameters and molecular number density. This can be done with proper mathematical treatment; but there must be a uniform set of assumptions and mathematical approaches.

6. Elterman's last recommendation for standardization concerns statistical treatment. Because the detected product of laser probing is a photon count, this gives the overall problem a distinct statistical character. The use of statistical parameters such as standard deviation, probable error, and so on should be an essential part of standards for laser probing.

If uniform measurement standards are set along the line of Elterman's six recommendations, then we can begin to collect a consistent body of data from many laser probers which, with time, will permit us to establish trends and to monitor long-term increases or decreases in upper-atmospheric pollutants.

OBSERVATIONS OF IONOSPHERIC MOVEMENTS BY THE USE OF A LARGE AERIAL ARRAY*

DR. B. H. BRIGGS, Department of Physics
University of Adelaide, South Australia

The ionosphere does not behave like a smooth mirror for radio waves, but more like an irregular diffracting screen. When a radio wave is reflected from it, a random diffraction pattern is formed over the ground. Simple arguments can be used to show that this pattern will move over the ground with a velocity which is twice the horizontal velocity of the ionosphere.(1) This phenomenon can be used for the detection of movements taking place in the ionosphere.

In the past, observations of the moving pattern have been made by the use of a small number of spaced radio aerials (usually three). The records obtained from such experiments are subjected to a complicated statistical analysis in order to derive the best estimate of the velocity of the pattern.(2) The statistical theories make certain assumptions about the nature of the movements, which are difficult to test. There has therefore been some uncertainty and controversy about what is really being measured in experiments of this type. In particular, it has been suggested that the movements may not be a bodily motion of the ionization, but rather some kind of wave which propagates through the ionosphere.(3)

In order to obtain more complete information about the nature of the movements, a new method of observation has been developed recently at the Buckland Park field station of the University of Adelaide. (Figure 1 illustrates the principle.) In this method, the radio diffraction pattern is sampled at 89 points, and converted into a visible pattern. The sampling is achieved by the use of an array of 89 radio aerials arranged as in Figure 2. Each aerial is connected by an underground coaxial cable to a radio receiver in a central laboratory. The output voltage from each receiver (which is proportional to the amplitude of a selected ionospheric echo) controls the brightness of a small lamp; thus the 89 lamps are arranged in a small array with the same configuration as the aerials. In order to obtain a

*This article has been adapted from a paper which originally appeared in the Proceedings of the Astronomical Society of Australia, Volume 1, No. 4 (December 1968), 150-151.

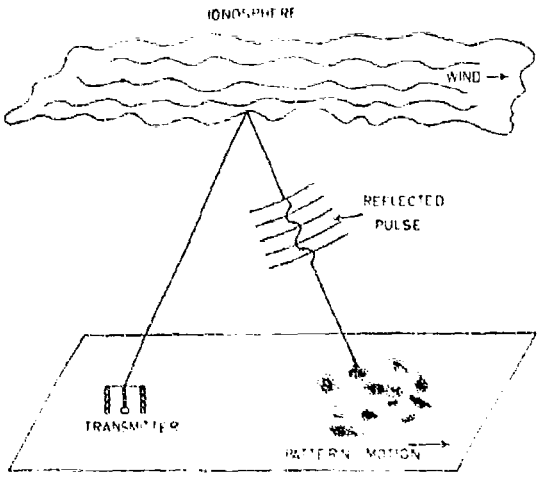

Figure 1. This diagram illustrates the principle of the method used to measure the horizontal drift velocity of the ionosphere.

smooth pattern, a diffusing screen is placed in front of the array of lamps.

Examples of the patterns obtained in this way are shown in Figure 3. These are successive photographs taken at intervals of 0.5s. The motion of the pattern from one to the next ("a" through "h") can be clearly seen. The field of view represents a circle on the ground with a diameter of 1 km. In order to study the movements visually, it is advantageous to speed them up rather than observe them in "real time." It has been found best to take successive photographs at intervals of 0.25s, and then to project the resulting 16-mm film at the standard rate of 24 frames per second. The movements are then speeded up by a factor of 6.

Preliminary results give some support to a "wave" interpretation--at any rate on some occasions. Ripple-like "wavefronts" are seen to cross the field of view in various directions, though with a preferred direction of movement on any one occasion. This behavior could arise from a bodily motion of the medium upon which there was superimposed a system of waves with a random azimuthal distribution of wave-normal directions.(3) However, further analysis is needed before any firm conclusions can be drawn.

For quantitative analysis, digital recordings of the data from the 89 channels will be made on magnetic tape. It will then be possible to evaluate on a computer the two-dimensional cross-correlation function between the patterns existing at two chosen instants of time. This function should have a maximum value at a point which represents the vectorial displacement of the pattern in the given time interval and, from this displacement, the pattern velocity can be deduced. It can be shown that this method avoids some of the arbitrary assumptions which were inherent in the earlier methods of correlation analysis, when applied to records from three aerials.(4) Also, more rapid variations of velocity can be studied.

The aerial array will also be used for other experiments in ionosphere and meteor physics, and for low-frequency radio astronomy.(5)

The project is supported by the General Physics Division of the Air Force Office of Scientific Research (OAR) under AFOSR Grant No. 864-67, the Australian Research Grants Committee, the Radio Research Board, and the University of Adelaide.

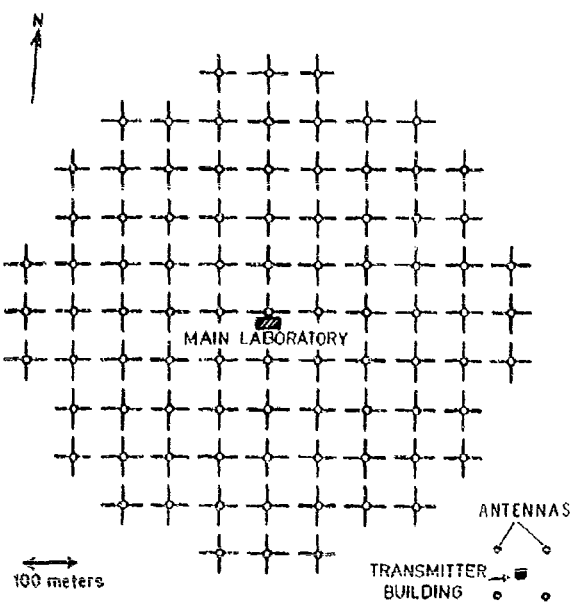

Figure 2. The arrangement of the 89 aerials of the receiving array and the associated transmitting aerials are shown in this diagram.

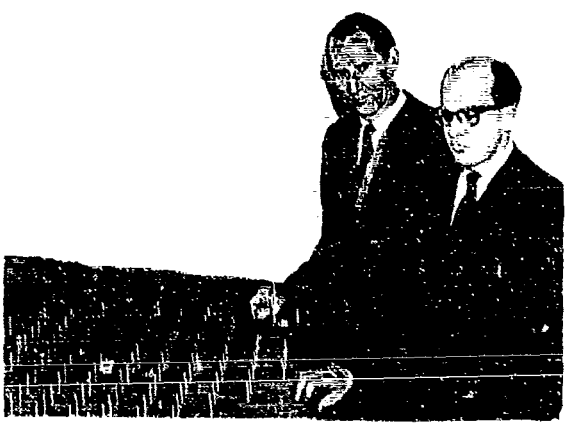

Dr. B. H. Briggs (right) and Dr. W. G. Elford (left), with a model of the aerial array. Dr. Elford is well known for his work on the radio observation of meteor trails, and is interested in the use of the array to extend this work to lower radio frequencies.

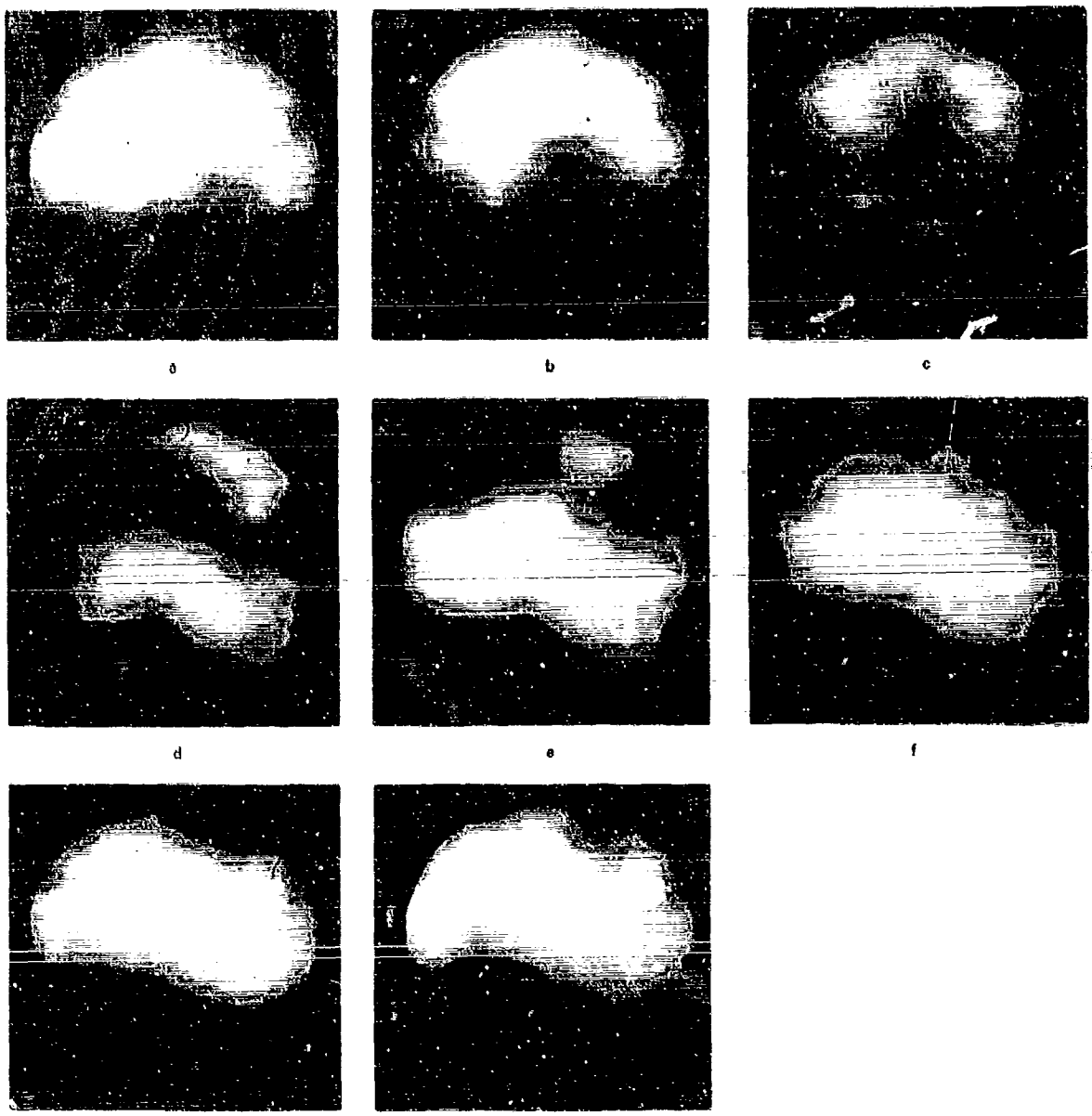

Figure 3. Photographs of the moving diffraction pattern taken at intervals of 0.5s. The field of view is 1 km in diameter.

REFERENCES

(1) Pawsey, J. L., *Proc. Camb. Phil. Soc.*, 31, 125 (1935).
(2) Briggs, B. H., G. J. Phillips, and D. H. Shinn, *Proc. Phys. Soc.*, B.63, 106 (1950).
(3) Hines, C. O., *Q. J. Roy. Met. Soc.*, 89, 1 (1963).
(4) Briggs, B. H., *J. Atmos. Terr. Phys.*, 30 (1968), 1777-1794.
(5) Briggs, B. H., W. G. Elford, D. C. Felgate, M. G. Golley, D. E. Rossiter, and J. W. Smith, "The Buckland Park Aerial Array." (to appear in *Nature*)

Dr. B. H. Briggs is with the Department of Physics, University of Adelaide, Adelaide, South Australia. He was educated at the Bradford Grammar School and at Cambridge University, both in England. He received his B.A. in 1945, his M.A. in 1948, and his Ph.D. in 1952.

Dr. Briggs has been an Assistant Director of Research in the Department of Physics, Cambridge University, and a Reader and Senior Lecturer in Physics at the University of Adelaide. He is a Fellow of the Institute of Physics and the Australian Institute of Physics, and a Member of the American Geophysical Union. He has a great many publications to his credit.

MAJOR ROGER A. GEESEY
Aerospace Mechanics Division
FJSRL

computational aspects of a unified approach to problems in estimation and detection

As technology advances along some "front," a level of sophistication is encountered which requires consideration of stochastic phenomena for refined analysis. In modern communication and control systems, the use of many techniques for statistical inference is now classical, with the major classifications for such techniques being decision theory and estimation theory. The general problem in decision theory is to perform an observation having a stochastic nature and to decide among the possible causes which produced it, while the estimation problem consists of determining values for parameters or processes of interest which are observed only remotely. (1)

It is usually possible to formulate a problem of statistical inference in communication or control as consisting of an observed process which is the sum of a signal process and a noise process. A comprehensive list of the important problems in estimation and detection which arise in modern systems employed by the Air Force would be too extensive to give here. They would include, however, the conventional communication and radar systems which are limited in power such that the received signal-to-noise ratio is unacceptable, and the guidance and control systems with accuracy limitations in basic components. In the more familiar problems, the signal is a known waveform (as in digital, synchronous communication systems), or else the signal is described by a few unknown parameters (as in some nonsynchronous communication, radar, sonar, and inertial systems). However, the more complex situation, in which the signal process itself is stochastic in nature, has more recently become of interest.

Communication systems now employ media such as troposcatter meteor trails or auroral and orbital chaff belts--randomly varying channels--which give rise to the reception of a stochastic signal. For purposes of secure communication, a message may be encoded by random processes, hence generating a stochastic signal detection problem for the receiver. In radar and sonar systems used against dispersive targets, the stochastic signal-detection problem again arises in processing returns. Radio telescopes and seismic detection systems utilize detectors for noise-like sources. Guidance and control systems, which are subject to time-varying disturbances, require an estimation of nonstationary stochastic processes to perform effectively in the disturbed environment. In estimation problems for control, the stochastic signal process is usually the plant output itself. Pattern recognition may also be formulated in terms of stochastic signal estimation by viewing the signal as the statistics of a data subclass.

As in all engineering which seeks a numerical answer to a physical problem, it is necessary to express a problem in terms of a mathematical formulation to which an effective mathematical theory can be applied to yield the desired numerical solution. It is not suggested that, in every case mentioned above, a mathematical formulation is known such that an existing theory is effective; but what is known is that a large class of such problems yields a formulation in which the signal and noise stochastic processes have known covariance functions in separable form. The separable form for a covariance function $R(t,s)$ consists of a finite linear combination of terms of the form

$$a(t)b(s),\ s \leq t;\ b(t)a(s),\ t < s$$

where the functions $a(\cdot)$, $b(\cdot)$ are dependent on only a single time variable. That such a covariance function is known includes the possibility that sufficient data is available to accurately determine the separable form by empirical methods.

The research conducted by the author at the Aerospace Mechanics Division, FJSRL, has determined mathematical techniques which are effective in solving both estimation and detection problems in terms of a formulation with separable covariances. (2,3) This research has enlarged the body of mathematical theory applicable to estimation and detection by allowing a less detailed problem formulation and by giving more effective digital computational methods for solutions. Also, the research has shown more clearly that the understructure for problems in estimation and detection is common to both, and consists of modeling an observed stochastic process as the output of a causal linear filter, driven by white noise, which is invertible on an arbitrary, finite-time interval. The significance of invertibility in such a model for an observed process is that the observation may then be easily "whitened," and the solutions for estimation and detection obtained by solving the simpler problem based on white-noise observations. "Whitening filter" techniques have been used previously, with large success, in engineering; this research has extended their utility to a broader problem formulation.

The modern Kalman-Bucy theory for estimation of nonstationary, Gauss-Markov processes has received widespread utilization. This theory is based on a problem formulation which includes a complete model for the signal process in the form of a finite dimensional linear system. But the problem of determining such a dynamical model from statistical information about the process has only recently been effectively solved; and it is the separable form for the covariance function which yields a process model to which the Kalman-Bucy theory is applicable. However, the research reported here has shown that, for a design based on the covariance function as data, the computational effort for solution to estimation problems

can be minimized by achieving invertibility in modeling and by using whitening filter techniques.

Although studies basic to detection theory preceded the groundwork for modern estimation theory by half a century, the solutions available in detection theory have remained difficult to implement in practical situations because analysis has been concentrated on integral equation formulations. But the solution for detection can be given, quite simply, by use of the whitening filter which results from an invertible model of the observations. So, as in the estimation problem, the key to solution is the appropriate model for the observation process, and the whitening filter techniques show that the essential aspect of solutions for both estimation and detection is the common modeling problem.

The desired invertible model and the resulting solutions for estimation and detection are obtained by an effective digital computational scheme for problems having the formulation in terms of separable covariances. This research has shown that a matrix differential equation of the Riccati type may be associated with the separable covariance to determine the invertible model. The initial value matrix Riccati equation, although nonlinear, has been extensively studied in estimation and control, and its familiarity makes this approach effective.

REFERENCES

(1) Van Trees, H. L., *Detection, Estimation and Modulation Theory*, New York: Wiley (1967).

(2) Greesey, R., "Canonical Representations of Second-Order Processes With Applications," *SRL 69-0001*.

(3) Geesey, R. and T. Kailath, "Applications of the Canonical Representation to Estimation and Detection in Colored Noise," *Proc. Symposium on Computer Processing in Communications*, Polytechnic Institute of Brooklyn, New York (1969). Published also as *SRL 69-0010*.

MASS SPECTROMETRIC STUDY OF LOW-FIELD MOBILITY, DIFFUSION, AND REACTIONS OF IONS IN GASES

DR. RALPH E. KELLEY
Directorate of Physical Sciences
AFOSR

At the Georgia Institute of Technology, Professors Earl W. McDaniel and David W. Martin have developed a unique drift tube mass-spectrometer apparatus (1) which is being used to study the drift velocities, diffusion, and reactions of ions in gases in low-to-moderate electric fields. This apparatus produces a high-resolution-time profile of the swarm of each distinct ion species present, as a function of the distance from the ion source. The pattern of ion-molecule reactions taking place is elucidated by comparison of the profiles for the species present at various gas pressures and drift distances.

Primary ions, which are produced directly in the ion source, are identified by their characteristic profile shapes; and, from the details of the shape, it can be determined whether the perturbing effects of any reactions are sufficiently small to permit a true drift velocity to be measured. For primary ions, techniques have already been developed to determine the longitudinal diffusion coefficient from the profile widths. Both the transverse diffusion coefficient and the rates of reactions which deplete the primary species can be found from the attenuation of the swarm with increasing drift distance.

For secondary species, true drift velocities can also be obtained when certain criteria, involving the details of the profile shapes, are met. All determinations are made over ranges of E/N, the ratio of electric-field strength to gas number density, which generally extend from small values, where the ions are essentially in thermal equilibrium with the gas, to values where the departure from equilibrium is considerable.

In addition to quantitative determinations of basic transport coefficients, the method has the important effect of permitting the identification of ion species present and the elucidation of the ion-molecule reaction patterns which prevail in various weakly ionized gases.

The quantitative determinations are of basic interest because comparisons of experimental values with theoretical calculations provide tests of postulated ion-molecule interaction potentials at separation distances greater than those which can be tested by the results of beam experiments. A knowledge of the way in which transport coefficients change with E/N is particularly useful in this regard. The coefficients enter also into basic calculations such as the rate of dispersion of ions by mutual repulsion, and the rate of ion recombination, processes which are important to the understanding of phenomena occurring in the upper atmosphere. The coefficients are of practical importance to the understanding of devices in which gas discharges occur, and to the solution of communications problems related to high-altitude explosions, rocket exhausts, and reentry trail ionization.

Information about ion-molecule reactions, both qualitative and quantitative, is particularly important for understanding the propagation characteristics of gaseous media such as the upper atmosphere and certain regions of space. The propagation characteristics are dependent on free-electron density which, in turn, is dependent on the molecular composition of the gaseous medium. The rate of electron-ion recombination is generally several orders of magnitude greater for molecular ions than for atomic ions. The nature and rates of ion-molecule reactions strongly affect the abundance of various molecular-ion species and, therefore, the electromagnetic propagation characteristics.

This research is supported jointly by the Office of Naval Research through Project SQUID and the General Physics Division of AFOSR.

REFERENCE

(1) Albritton, D. L., T. M. Miller, D. W. Martin and E. W. McDaniel, *Phys. Rev.*, 171, No. 1 (1968), 94.

search for a third-order phase transition in water

DR. GEORGE O. ZIMMERMAN
Physics Department, Boston University

Of the three classical states of matter—gases, liquids and solids—the liquid state is the hardest to depict on a microscopic or molecular scale. While an ideal gas could be depicted as an assembly of molecules with a perfectly random distribution in space as well as in velocity (as long as some boundary conditions are satisfied, e.g., the average energy is constant, no molecules are allowed outside an enclosure if the gas is confined in a container, etc.), and while an ideal solid could be depicted as a perfectly spatially ordered array of molecules, a liquid is depicted as something between those two.

Methods of statistical physics based on the concept of random distribution, with intermolecular forces added as a perturbation, are highly successful in the treatment of real gases. Theoretical methods of solid-state physics, based on the idea of an ordered molecular state, with some imperfections due to thermal, zero-point, and other excitations added as perturbation, are similarly successful in treating solids. Liquids are treated alternately as partially ordered gases or as very rare and disordered solids. (1) In the latter case, the liquid is considered as a solid with vacancies whose size is of the order of molecular volume, and the fraction of vacancies per mole can be defined as $(V - V_S)/V$ where V and V_S are the molar volumes of the liquid and solid, respectively, taken at the melting point.

The true molecular picture is undoubtedly somewhere between the two extremes, with the proximity to either dependent on the temperature. According to Rice,(1) at temperatures above but near the melting temperature, the long-range order inherent in a solid is destroyed; but the short-range order, on the scale of a few molecular diameters, still persists. At higher temperatures, this short-range order is gradually eliminated until, at the boiling point, we have a mainly disordered array. The amount of order can be described by a correlation function, g(r), which describes the relative density of molecules as a function of the distance r. It is here assumed that g(r) is an isotropic function, independent of the polar angles θ and φ. Once this function and the energy of interaction between molecules as a function of distance are known, one can calculate macroscopic properties of a substance which can be determined experimentally. It is very hard to calculate g(r) except in some very simple cases. It can, however, be determined from X-ray diffraction experiments or from measurements of macroscopic quantities. In the latter determination, g(r) plays the role of an adjustable parameter.

Water, although one of the most abundant liquids on this planet, is also one of the least typical and consequently hardest to understand. To begin with, the specific volume of water contracts upon melting and goes through a minimum at about 4° C, which corresponds to a density maximum. Were one to simply calculate the fraction of vacancies in the liquid, $(V - V_S)/V$, a negative number would result. A related phenomenon is that, in ice-water mixtures at the melting point, the fraction of the solid is decreased with increasing pressure, while in most substances it increases.

Among other atypical properties of water are its high specific heat and, as will be shown later, when the results of our sound velocity measurements are discussed, its adiabatic compressibility. The adiabatic compressibility is defined as the fractional change of the density upon application of pressure at constant entropy. In thermodynamic notation, it is $\frac{1}{\rho}\left(\frac{\partial \rho}{\partial p}\right)_S$ where ρ, p, and S are the density, pressure, and entropy, respectively. The adiabatic compressibility of water is a monotonically decreasing function of temperature from 0° to about 74° C, where it has a minimum and then increases to infinity at the critical point. The remarkable fact about this is that water becomes stiffer, or more resistant to compression, as temperature increases (i.e., the density change in water per unit change in pressure decreases between 0° and 74° C). Thus, it seems that there are more vacancies in the solid, ice, into which molecules can go, when pressure is applied with a consequent change in density, than there are in the liquid. In "normal" liquids, compressibility increases with temperature. The atypical properties of water mentioned above, and others, have to be explained if one considers the molecular theory of water.

Several theories of the molecular structure of water have been advanced; the most quoted are those of Bernal and Fowler,(2) Euken,(3) and Pople.(4) The starting point of each is the molecule itself, which can be described as a triangle with the center of the negatively charged oxygen ion at its apex, and two positively charged hydrogen ions making an angle of 109° (the actual experimental determination shows 105°). The water molecule will thus possess a permanent electric dipole moment, with the negative charge near the oxygen and the positive charges near the hydrogens; consequently, it is a polar molecule. Because the water molecule is polar, it will attract other polar molecules and therefore becomes the good solvent that it is. Because it is a polar molecule, it will attract other water molecules,

thus forming aggregates in the liquid. In such an aggregate, the positively charged hydrogen atom of one molecule will be attracted to the negatively charged oxygen atom of another molecule, thus forming a hydrogen bond.

The situation becomes somewhat more complicated if we consider that the hydrogen atom can detach itself from an oxygen atom, leaving a hydroxyl molecule behind and forming a positively charged complex with other water molecules. Experiments show that the average time a hydrogen atom can be associated with a particular water molecule in the liquid is of the order of 10^{-13} second.

If, however, we consider the water molecule as a stable entity, we can describe the liquid, as Bernal and Fowler(2) do, as a mixture of 2 aggregates. One is an aggregate of 4 molecules, arranged as a tetrahedron where the hydrogen atom of one always points at the oxygen of its neighbor. This structure is loosely packed and has a molar volume of about 19.5 cc, as compared to closely packed single water molecules whose molar volume can be calculated to be 6.6 cc. Another denser structure, also an aggregate of 4 molecules but now in a rhombohedral arrangement with a molar volume of 16.7 cc, is also present. The fraction of each species of aggregate in water is a function of temperature. The density maximum at 4° C is explained by the gradual change of the tetrahedral structure into the rhombohedral, superimposed on the thermal expansion of both structures. Thus, a process which increases the density with increasing temperature, superimposed on a process which decreases the density with temperature, will generally result in a maximum if the two processes are different functions of temperature.

The two aggregates correspond to the structures of ice I and ice II, respectively. Recently, Erlander(5) suggested the existence of a different species of water formed of rhombohedral aggregates only, with different physical properties from those of ordinary water. He calls the new species superwater.

Euken(3) suggests that the liquid phase of water consists of four kinds of aggregates whose concentrations vary with temperature. The four kinds are single molecules, H_2O; two molecular, $(H_2O)_2$; four molecular, $(H_2O)_4$; and eight molecular, $(H_2O)_8$ -clusters with different volumes per molecule and different energies of dissociation. Those would account for the high specific heat of water.

The third picture, proposed by Pople,(4) agrees with that of Bernal and Fowler insofar as the existence of different aggregates is acknowledged; but the density behavior is not explained by the change in the fractional composition of aggregates with temperature. Instead, the explanation is that the hydrogen bonds become more flexible with temperature, thus allowing the aggregates to interpenetrate. This explains the density maximum at 4°.

The supposition common to the first two theories, that of Bernal and Fowler, and that of Euken, is that the properties of water can be explained by the transformation of aggregates into each other as a function of temperature. The view of this process, given above, is somewhat simplistic since it assumed that the aggregates are permanent structures. In reality, the aggregates are evanescent structures which constantly form and break up. Any one molecule is associated with any one aggregate for only a very short time. However, a certain number of aggregates exist at any instant, so that one can describe water as consisting of a certain number, an average number, of aggregates.

A change in the average proportion of one kind of aggregate as a function of temperature might show up at certain temperatures as a third-order phase transition.

According to the classification of phase transitions, the N'th order transition is defined such that a discontinuity appears in the N'th order derivative of the Gibbs free energy. The Gibbs free energy is defined as

$$G = U - TS + PV$$

where U is the internal energy, T the absolute temperature, S the entropy, P the pressure, and V the volume.

$$dG = dU - TdS - SdT + PdV + VdP = -SdT + VdP$$

There are two first derivatives of G with respect to its natural variables P and T.

$$\left(\frac{\partial G}{\partial T}\right)_P = -S \quad \text{and} \quad \left(\frac{\partial G}{\partial P}\right)_T = V.$$

In a first-order phase transition, examples of which are the solid-liquid and liquid-vapor transition, usually both S and V are discontinuous. There are three second-order derivatives of G

$$\left(\frac{\partial S}{\partial T}\right)_P = \frac{C_P}{T}$$

where C_P is the specific heat at constant pressure,

$$\left(\frac{\partial V}{\partial P}\right)_T = -V\kappa_T = \rho\kappa_T$$

where κ_T is the isothermal compressibility, and

$$\left(\frac{\partial V}{\partial T}\right)_P = V\alpha_P$$

where α_P is the thermal expansion coefficient at constant pressure.

Discontinuities in any of the second-order derivatives define a second-order phase transition. Examples of second-order phase transitions are the transition at a critical point, the superconducting transition at zero magnetic field, and the superfluid transition in liquid helium. A cusp or kink in any of the second-order derivatives would denote a discontinuity in a third-order derivative, and thus indicate a third-order phase transition.

W. Drost-Hansen(6) made a survey of experimental data on water and claims to have observed such kinks in several measured properties of water, among them the viscosity and dielectric constant. He claims that these discontinuities occur at approximately 15°, 30°, 45°, and

60° C. On the other hand, M. Falk and G. S. Kell(7) have examined data on the physical properties of water where discontinuities or kinks were reported. Among the properties examined were the vibrational spectrum, compressibility, surface tension, viscosity, and others. They claim that the discontinuities are spurious and within the scatter of the data. It is indeed instructive to plot some quantities and see how such kinks or discontinuities could have been inferred.

Figure 1 is a graph of the temperature derivative of the specific heat, obtained from the specific heat data given in the Chemical Rubber Company's *Handbook of Chemistry and Physics*.(8) One could imagine discontinuities at several temperatures; however, those are within the precision of the data, so that no definite conclusion can be drawn about their existence. Another example is shown in Figure 2 where the isothermal compressibility of Kell and Whalley(9) and that of Greenspan and Tschiegg(10) have been plotted. No smooth curve can be drawn through the centers of the points of Kell and Whalley between 40° and 70° C. This would suggest a kink in the quantity. However, the smooth curve is displaced by only the width of the error in the point; thus, this suggestion cannot be taken seriously.

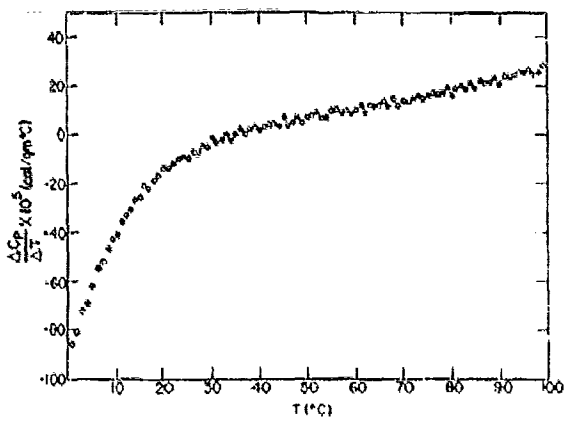

Figure 1. $\Delta C_p/\Delta T \simeq \frac{\partial C_p}{\partial T}$ obtained by taking the differences between specific-heat values one degree apart. The specific heat is taken from the CRC Handbook.(8)

Several investigators(9,11) have looked for these discontinuities or kinks, and report no discontinuities outside the scatter of their data. Those investigations have, however, taken relatively few points in any given temperature range, and a kink or discontinuity, if its effect extended over less than one degree, could have been overlooked. Because it is possible to measure the velocity of sound with great precision, we decided to search for kinks in the velocity of sound in water.

The velocity of sound, u, is related to the adiabatic compressibility κ_S by

$$u^2 = \left(\frac{\partial P}{\partial \rho}\right)_S = \frac{1}{\rho \kappa_S}$$

κ_S is in turn related to κ_T by

$$\kappa_T = \gamma \kappa_S$$

where γ is the ratio of the specific heat at constant pressure to that at constant volume. A kink in κ_T or γ would indicate a third-order phase transition.

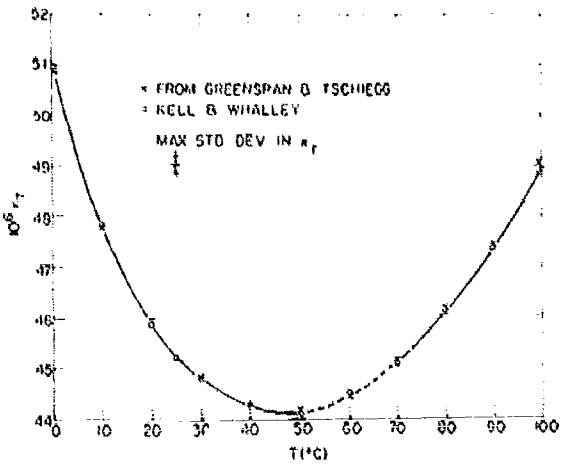

Figure 2. Isothermal compressibility κ_T, in units of per bar, as given in references 9 and 10.

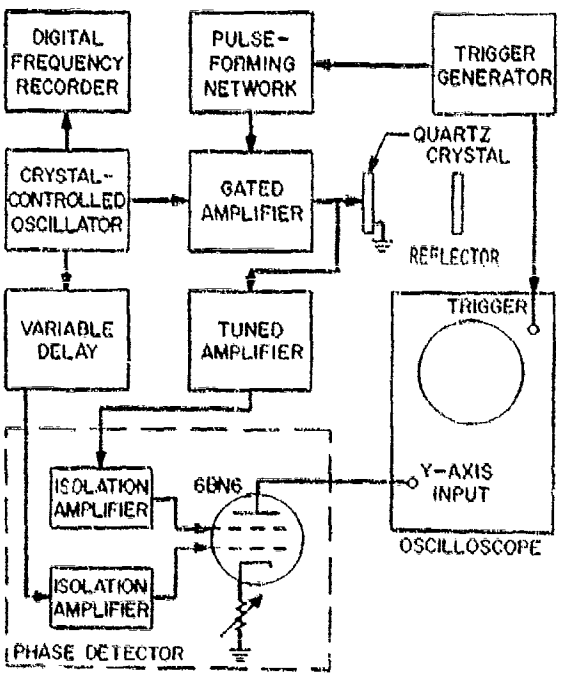

Figure 3. Block diagram of the electronic apparatus for sound velocity measurements.

Although the velocity of sound in water has been measured by others, the number of points in any temperature range was small. We have taken 2300 points in the temperature range between 3° and 80° C.(12) The measurements were carried out by immersing a quartz transducer tuned to 10 MHz (which also served as a receiver), and a reflector parallel to the transducer, in distilled water contained in a vacuum flask. The water was stirred continuously to maintain temperature uniformity. The temperature was measured by means of a platinum resistor.

The velocity of sound was measured by a pulsed phase comparison technique(13) A block diagram of the electronics is shown in Figure 3. In this method, the phase of the sine wave of a received echo is brought into coincidence with that of a continuously running master oscillator by delaying the oscillator wave by means of an adjustable delay line. In our apparatus, the first echo was received at about 100 microseconds after the transmitted pulse, while the time resolution of the apparatus was 0.2 nanosecond.

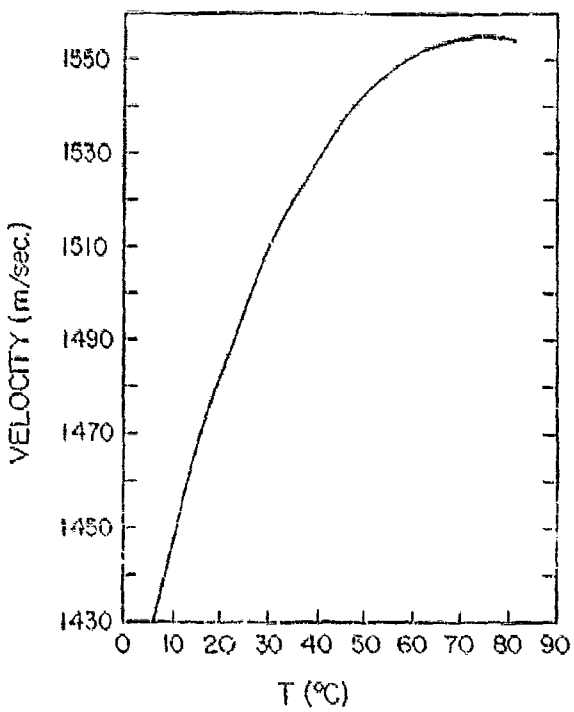

Figure 4. Velocity of sound as a function of temperature.

Figure 4 shows the velocity of sound in water as a function of temperature. No scatter can be observed on this scale. One should notice that the maximum occurs at 74° C, corresponding to a minimum in κ_S. In order to detect the presence of any discontinuities or kinks, the data was fitted to polynomials in temperature of the form

$$u = \sum_{n=0}^{N} A_n T^n$$

and the deviations of the points were plotted. This is shown in Figure 5 for N = 2, 4, 6, and 8. The main contribution to the deviations in the fit to the N = 8 polynomial, where the velocity in meters per second is given by

$$u = 1403.44 + 4.79242T - 3.22874 \times 10^{-2}T^2$$
$$- 1.18815 \times 10^{-3}T^3 + 4.97534 \times 10^{-5}T^4$$
$$- 1.00377 \times 10^{-6}T^5 + 1.14662 \times 10^{-8}T^6$$
$$- 7.02210 \times 10^{-11}T^7 + 1.79249 \times 10^{-13}T^8$$

is due to temperature inhomogeneities in the water. It can be seen from Figure 5 that no anomalies greater than 35 ppm exist. This is within the scatter of our data. One could not, however, exclude the possibility of kinks at 20°, 25°, 32°, 38°, and 47° C. In our opinion, the deviations from the fit

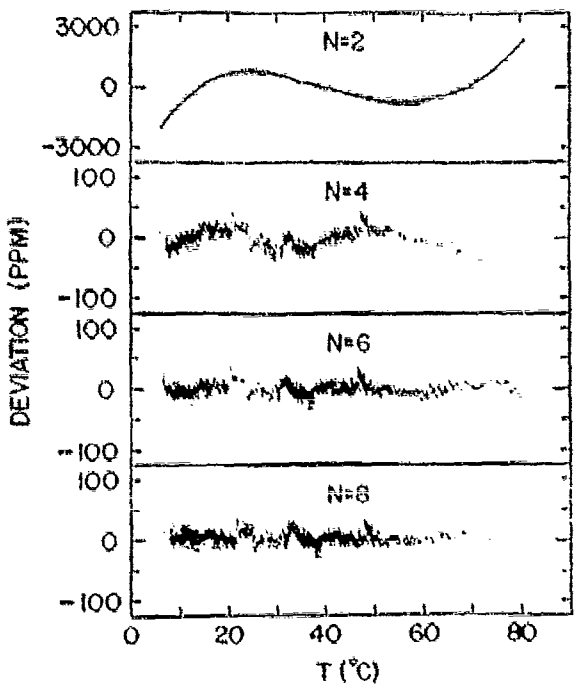

Figure 5. Deviations, in parts per million, from the least squares fits to N = 2,4,6, and 8.

are spurious and caused by our experimental uncertainities.

The question of the existence of discontinuities or kinks in water will have to be resolved by more precise measurements. However, even then, people could infer either the existence or nonexistence of anomalies because no experiment can be performed with infinite precision, and one needs that to prove the absence of a phenomenon. Thus, the question of the structure and properties of water, the most abundant and most atypical liquid on earth, will

be with us for some time to come.

REFERENCES

(1) Eyring, H., J. Hildebrand and S. Rice, "The Liquid State," *International Science and Technology*, (March 1963), 56.
(2) Bernal, J. D. and R. H. Fowler, *J. Chem. Phys.* 1 (1933), 515.
(3) Luken, A., *Z. Electrochem.*, 52 (1948), 255.
(4) Pople, J. A., *Proc. Roy. Soc.*, A 205 (1951), 163.
(5) Erlander, S. R., "Structure of Superwater," *Phys. Rev. Letters*, 22, 5 (1969), 177.
(6) Drost-Hansen, W., "The Puzzle of Water," *International Science and Technology* (Oct 1966), 86.
(7) Falk, M. and G. S. Kell, "Thermal Properties of Water: Discontinuities Questioned," *Science*, 154 (1966), 1013.
(8) "Specific Heat of Water," *Handbook of Chemistry and Physics*, Cleveland, Ohio: Chemical Rubber Co., (1968), D94.
(9) Kell, G. S. and E. Whalley, *Phil. Trans Roy. Soc.*, London, A258 (1965), 565.
(10) Greenspan, M. and C. E. Tschiegg, *J. Research Natl. Bur. Std.*, U.S., 59 (1957), 249; *J. Acoust. Soc. Am.*, 31 (1969), 75.
(11) Ruscke, E. W. and W. B. Good, "Search for Discontinuities in the Temperature Dependence of the Dielectric Constant of Pure Water from -5° to +25°C," *J. Chem. Phys.*, 45 (1966), 4667.
(12) Senghaphan, W., G. O. Zimmerman and C. E. Chase, *J. Chem. Phys.* (to be published)
(13) Chase, C. E., "Propagation of Ordinary Sound in Liquid Helium near the λ Point," *Phys. of Fluids*, 1 (1958), 193; Whitney, W. M. and C. E. Chase, "Ultrasonic Velocity and Dispersion in Liquid Helium II from 0.15 to 1.8°K," *Phys. Rev.*, 158 (1967), 200.

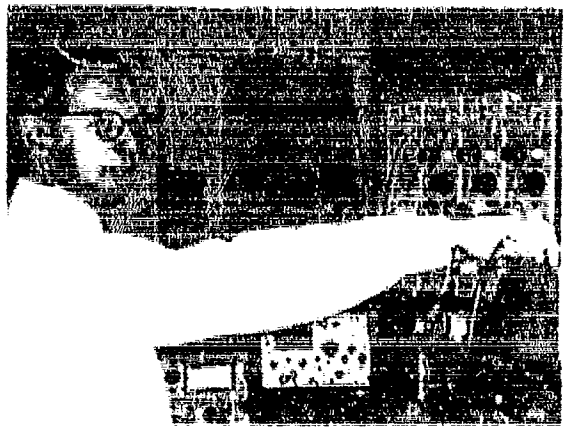

Dr. George O. Zimmerman is an Associate Professor of Physics at Boston University, and a visiting scientist at the M.I.T. Francis Bitter National Magnet Laboratory. He received his B.S., M.S., and Ph.D. from Yale University—the Ph.D. in 1968.

In 1963, Dr. Zimmerman joined the staff of Boston University, where he conducts research in low-temperature physics. The measurement of the velocity of sound in water, reported here, was suggested by Dr. C. E. Chase of the Francis Bitter National Magnet Laboratory to whom the author is indebted for many suggestions and calculations. Some of the results reported here are to be published in collaboration with Dr. Chase.

Professor Zimmerman's investigation of helium-3 and magnetic systems at low temperatures is sponsored by the AFOSR Solid State Sciences Division under grant AF-AFOSR-69-1770.

The Biochemistry of Learning and Memory

DR. HARVEY E. SAVELY
Director of Life Sciences, AFOSR

Over a 10-year period beginning in 1959, the Air Force Office of Scientific Research has supported research by Professor Holger Hydén at the University of Goteborg on biochemical changes that can be detected in nerve cells after learning. Professor Hydén was able to consider a problem of this kind because he had developed techniques for biochemical analyses of single cells. This required not only extreme manual dexterity in teasing out single cells, but also new micromethods for dealing with the small mass of a cell. In 1959 Professor Hydén was just beginning this line of work, which was received quite skeptically at the time by some neurophysiologists.

Another application of this technique has been to study the interrelation between neurons (nerve cells) and glia, which are the cells that surround the neurons everywhere. In the brain, for example, the glia are 10 times as numerous as nerve cells and constitute more than 50% of the total mass. Hydén assumed that such a pervasive association surely implied something more than just mechanical support, and that the function of the neuron probably depended in important ways on biochemical processes in the glia.

Over the last 10 years Professor Hydén and his colleagues have published 62 papers dealing with these two research themes.

The biochemical correlates of learning were sought in the hippocampus of the brain (a region known to be active in learning) in rats trained to change from right-handedness to left-handedness. It was shown that the synthesis of two acidic protein fractions increased during training, and that this was related to the learning process. An analysis for ribonucleic acid (RNA) in the neurons in a control center for the transfer of handedness, located in the brain cortex, showed that the increased synthesis was associated with the reversal of handedness. Similar changes were also found in brain centers linked to the vestibular apparatus, which provides sensory input for balancing and spacial orientation, in animals subjected to new experiences stimulating these systems.

The neuron-glia interactions have been shown by an analysis of adjacent nerve and glia cells that have been teased apart. Analyses of enzyme activity, RNA, and protein content reveal that the neuron is dominant from an energy-requirement point of view. Rhythmic changes could be shown in

neurons and glia in the reticular formation of the brain during transition from sleep to wakefulness. Changes in the base ratios of RNA in the glia in the globus pallidus preceded similar changes in their associated neurons in Parkinson's disease (a form of palsy in man associated with changes in specific brain nuclei such as the globus pallidus).

In general, the neuron and its associated glia were found to form a physiological unit where the glia show a more rapid turnover of RNA and protein and are apt to take to anaerobic glycolysis under changed conditions; on the other hand, the neuron under the same conditions would increase the utilization of energy by way of the respiratory biochemical chain.

Professor Hydén's studies have stimulated a widespread interest in the biochemistry of learning and memory. A number of his findings have now been confirmed in several laboratories. All of this is but a first step on what will ultimately lead to powerful insights into the brain mechanisms that underlie learning and memory. One line of investigation will undoubtedly proceed toward possible changes in these mechanisms by drugs. Another line is already pointing toward a study of the effects of nutrition and toxic substances on the brain during critical periods of its development before and after birth. Professor Hydén's contributions and his stimulation of biochemical analysis at the cellular level will be a significant landmark in this adventure.

REFERENCES

(1) Hydén, H., "RNA in Brain Cells," *The Neurosciences*, G. C. Quarton, T. Melnechuk and F. O. Schmitt, eds., New York: The Rockefeller University Press, 1967.

(2) Hydén, H. and P. W. Lange, "Brain Cell Protein Synthesis Specifically Related to Learning," *Proc. Nat. Acad. Sci.* (In press)

(3) Hydén, H., *Biochemical Aspects of Learning and Memory in the Human Mind*, Amsterdam: North-Holland Publishing Co., 1967.

INSTITUT DE SAINT LOUIS: *German-French Research Cooperation**

LT COL RICHARD T. BOVERIE, EOAR

The Institut de Saint Louis (I.S.L.) in the town of St. Louis, France on the French-German border (see Figure 1) was formally established effective 22 June 1959 in accordance with an agreement signed by the West German and French Governments on 31 March 1958. Its mission, as stated in the agreement, was to seek "close cooperation of scientific and technical research and development in armament to strengthen the defense of their countries." By

** Project Officers from the European Office of Aerospace Research periodically visit various research institutions in Europe, the Middle East, India, and Africa. These visits are made to identify current foreign research programs of possible use to Air Force scientists. Such information often leads to the establishment of working relationships between foreign and U.S. Air Force scientists. This article briefly describes one important institution visited recently.*

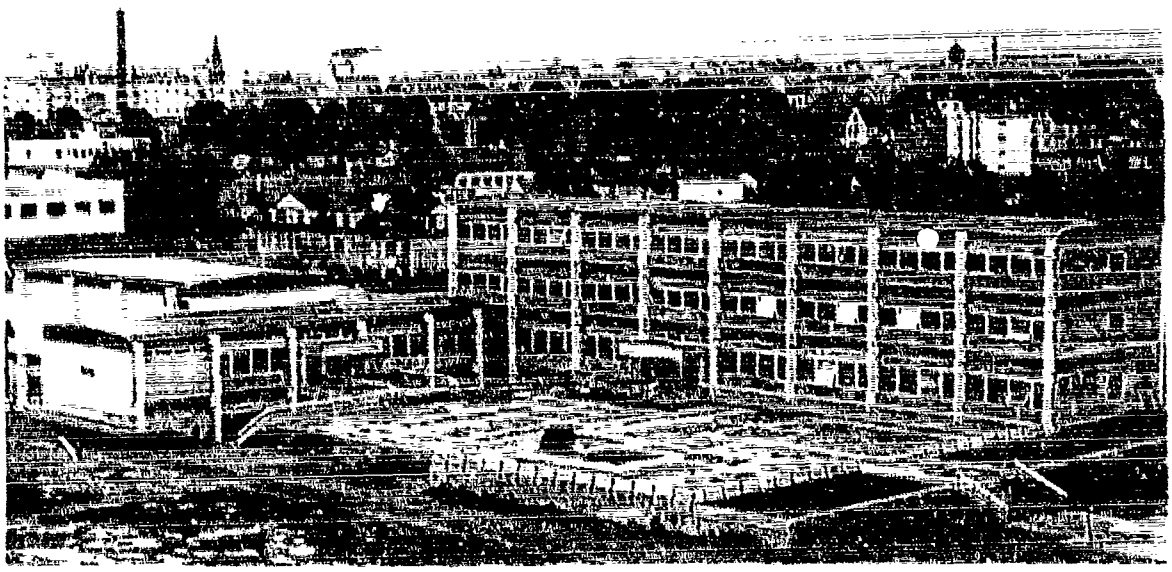

Figure 1. Main entrance of I.S.L.

agreement, the Institut is referred to in German as the "Deutsch-Französiches Forschungsinstitut," and in French as the "Institut Franco-Allemand de Recherches," but quite often simply as the "Institut de Saint Louis." Essentially, I.S.L. is active in cooperative research in such areas as hypersonic flow, shock waves, and ballistics.

West Germany and France contribute equally to the investment and maintenance costs of I.S.L., which has a staff of 465 people, 92 of whom have scientific or engineering degrees. The Institute is managed jointly by Ing. en Chef d'Armement A. Auriol as the French Co-Director, and Dr. R. Schall as the German Co-Director. Major facilities include a hypersonic shock tube, a hypersonic tunnel, a high-velocity light gas gun (projectile velocities up to 10,000 meters/sec), conventional powder guns with projectile velocities up to 3,000 meters/sec, special measurement and instrumentation devices, and an IBM 360/40 computer.

Although I.S.L. is primarily oriented towards defense research for France and West Germany, it welcomes research association with the United States and other countries having mutual defense problems.

I.S.L. has developed an extensive capability in the investigation of fast processes by photographic techniques embodying electric spark, X-ray flash, and pulsed-type laser illumination. Twenty-four spark shots can be made at nanosecond intervals, with the result that high-velocity-projectile travel of only a few millimeters takes place between shots. A recent improvement in this system permits the acquisition of as many as 5,000 pictures. This process has been used to examine the puncture of armor plate (see Figure 2); a burning methyl-alcohol droplet in the presence of a shock (the shock wave and wake tear the flame from the droplet, which itself is deformed); and a bullet moving at high velocity into an exploding gas mixture, with periodic detonation of the gas ahead of the bullet.

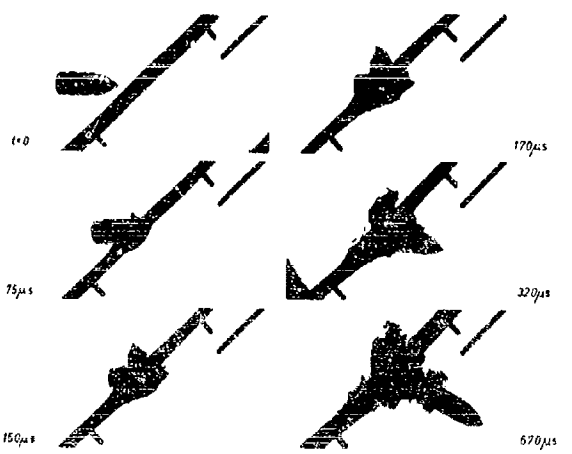

Figure 2. Penetration of an armour plate (8.5 mm, R=90 kp/mm²); caliber 20 mm, impact velocity 420 m/s; taken with a 24-spark camera.

Figure 3. X-ray-flash photography of a copper rod (3 mm Ø, 60 mm long) penetrating an aluminum target; impact speed: 1000 m/s.

A sample of X-ray flash photography may be seen in Figure 3 which shows a copper rod penetrating an aluminum target at a speed of 1,000 meters/second. Also, Figure 4 shows the jet formation of a shaped charge in a sequence of flash radiographs. Shadowgraphs of a 9-mm sphere fired into an oxygen-air mixture at 1,900 m/s, and of a model fired in atmospheric air at M = 1.8, are shown in Figures 5 and 6, respectively.

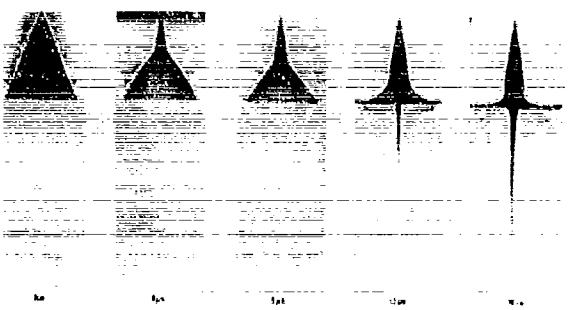

Figure 4. Jet formation of a shaped charge (sequence of flash radiographs).

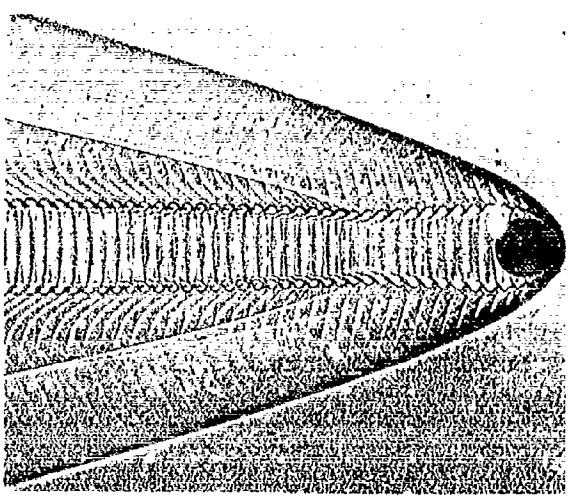

Figure 5. Shadowgraph of 9-mm sphere fired into an oxygen-air mixture at 1900 m/s.

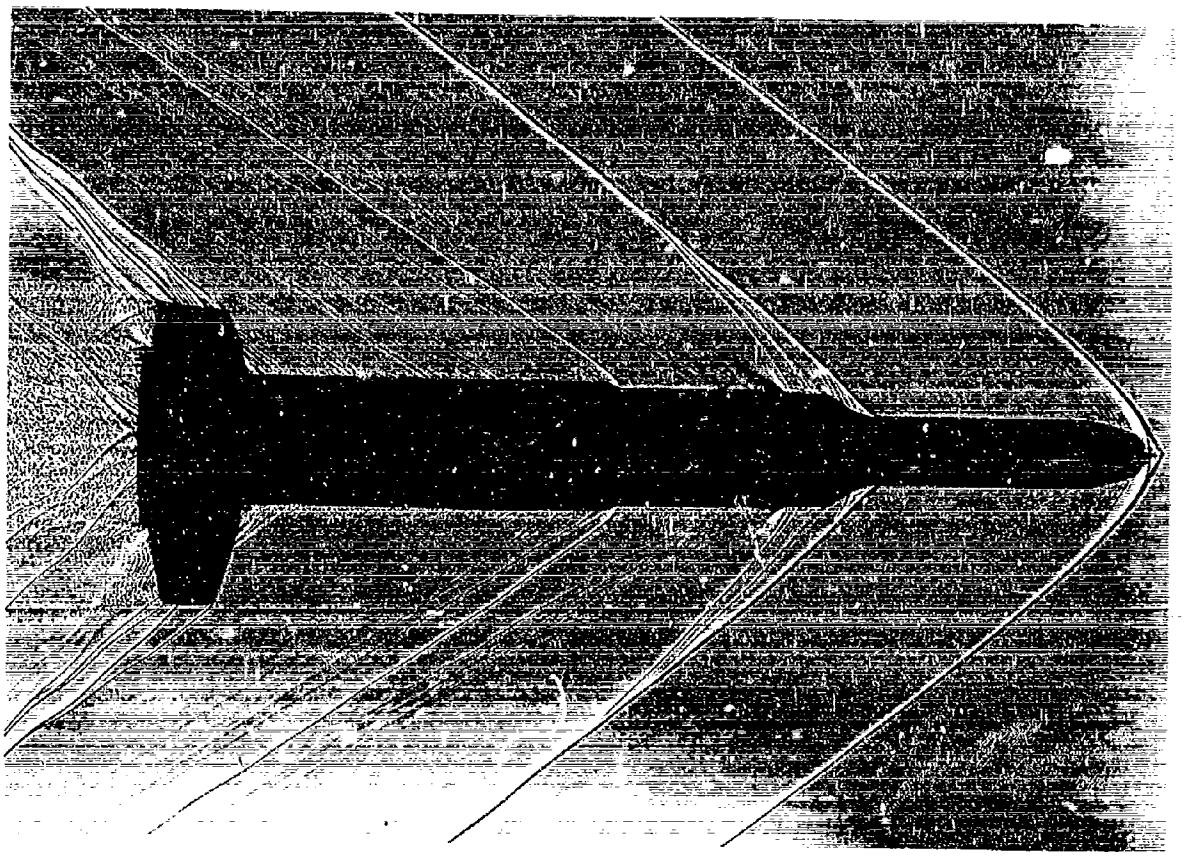

Figure 6. Shadowgraph of a model fired in atmospheric air at M = 1.8.

To analyze trajectories, 90-mm caliber models are fired, with their behavior determined by photographic records made at 16 positions, and with two orthogonal views at each position. Velocity profiles are established through the use of microwave and Doppler-effect techniques utilizing special initial-velocity and radar instrumentation developed at I.S.L.

The expansion and effect of strong and weak shock waves, with particular emphasis on the sonic boom, are under continual study at I.S.L. One recent study was centered on the quantitative analysis of sonic-boom focusing phenomena. As a preliminary approach to the problem, the refraction of low-intensity stationary shock waves in a nonhomogeneous atmosphere was studied. This investigation was restricted to the simple cases of the two-dimensional propagation of an N-shaped wave in an axisymmetrical atmosphere, and of a step wave in a stratified atmosphere. Calculation methods were based on shock properties. The refraction of a step wave was described by a differential equation for which approximate solutions can be found. The numerical results obtained correlate well with flight-test data.

In addition to work in ballistics, where the behavior of projectiles from launch to impact is being investigated, and research in aerodynamics concerned with hypersonic phenomena (between Mach 5 and Mach 15), such as encountered by reentry vehicles, I.S.L. is conducting investigations in: the composition of the upper atmosphere, using mass-spectroscopy methods; flame propagation and supersonic combustion; the detonation of gases and explosives; the expansion and effect of weak and strong shock waves; the behavior of materials subjected to the stresses of an explosion; holography; and the chemistry and mechanics of explosive materials.

ACKNOWLEDGMENT

The author is indebted to Professor Dr. R. E. Kutterer (former German Co-Director) and Dr. Schall for information on which this article was based to a large extent, and to Ing.en Chef d'Armement Auriol and Dr. Schall for reviewing the original manuscript of the article.

DOUBLE-QUANTUM DETECTION OF MICROWAVE SOUND

DR. PAUL H. CARR
and
ALAN J. BUDREAU
Microwave Physics Laboratory, AFCRL

The low velocity of sound as compared with that of electromagnetic radiation has motivated research into sonic delay lines as compact solid-state devices useful in radar signal processing, calibration, and other functions. It is possible to operate such devices at microwave frequencies. The interaction of sound at such frequencies (100 MHz to tens of GHz) with materials is also of considerable scientific interest, permitting the study of energy levels and elastic constants. These sound waves are generated piezoelectrically from electromagnetic waves of the same frequency, using either a vacuum-deposited thin film of piezoelectric material, such as cadmium sulfide, or by using an appropriately oriented piezoelectric material as the sample.

In the past, detection has generally been by the inverse of the same process, producing electromagnetic signals, which can then be processed by standard radar techniques. There are disadvantages to this approach. It is phase-sensitive, so that a wave arriving at a slight angle to the detecting surface (due to the nonparallelism of the detecting and generating surfaces) will partially cancel itself out, leading to a weakened signal and therefore an erroneous estimation of its strength. Parallelism is particularly difficult to obtain in the GHz range, since the sonic wavelengths are comparable to those of light. A further disadvantage is that, for volume or bulk waves, piezoelectric detection can only occur at the sample end, committing the builder of a delay line to a single delay determined by the length of the sample.

A new method, double-quantum detection, overcomes these disadvantages. In the presence of a magnetic field, various paramagnetic ions which can be added to a crystal by doping undergo energy-level splitting. The quantum theory of such a system reveals that the crystal can absorb sound energy plus electromagnetic energy as a part of the same process, provided that their sum is equal to the line splitting. (See Figure 1) Thus a

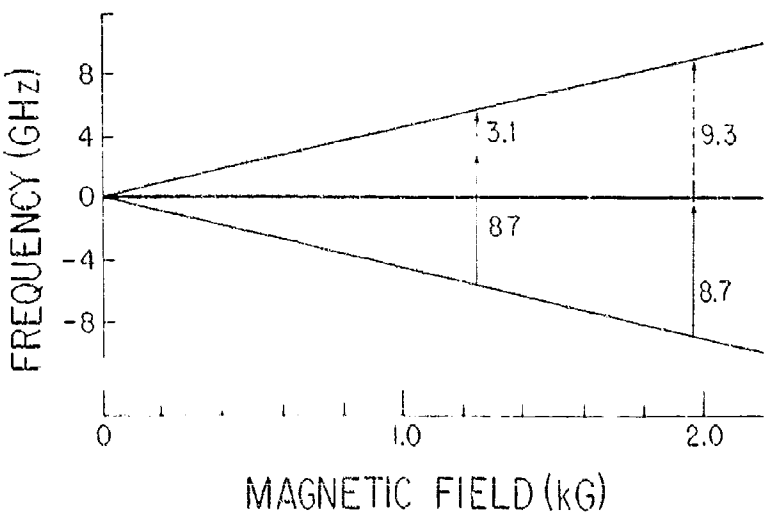

Figure 1. Energy level diagram of double-quantum detection. The sloping lines and the central line represent the splitting of the energy levels of a paramagnetic ion, here ferrous iron, as a function of magnetic field. Detection of phonons of 3.1 and 9.3 GHz, both using 8.7 GHz continuous-wave photons, is shown.

quantum of sound (phonon) plus a quantum of electromagnetic energy (photon) which *together* have an energy equal to the energy gap are absorbed in a single event. Hence the descriptive term, double-quantum (DQ) detection. In practice, at a given magnetic field, the absorption of a continuous-wave (CW) electromagnetic wave by the sample is monitored. When a phonon arrives, it provides the additional energy required for the DQ process, and an increased absorption of the CW signal occurs. Thus, the presence of the sound signal affects the intensity of an electromagnetic wave, without the need for piezoelectric conversion.

In these experiments, microwave pulses from a magnetron were fed to a resonant cavity containing a cadmium-sulfide piezoelectric film transducer on the end of a magnesium-oxide rod, as shown in Figure 2. The CdS film generated phonons which traveled along the rod and were reflected back and forth from the ends. Thus a single pulse propagated many times the length of the rod. The detector consisted of a sapphire-loaded cavity resonant at 8.7 GHz. The reflection of photons at this frequency was monitored, and in the appropriate magnetic field produced a signal for each phonon pulse. The paramagnetic ion was provided by doping with ferrous ions. Note that the detector is not necessarily at the end of the sample rod, and can even be moved mechanically to provide a variable delay.

The insensitivity of the DQ detector phase eliminated the poor decay pattern frequently seen in attenuation experiments (Figure 3), and thereby

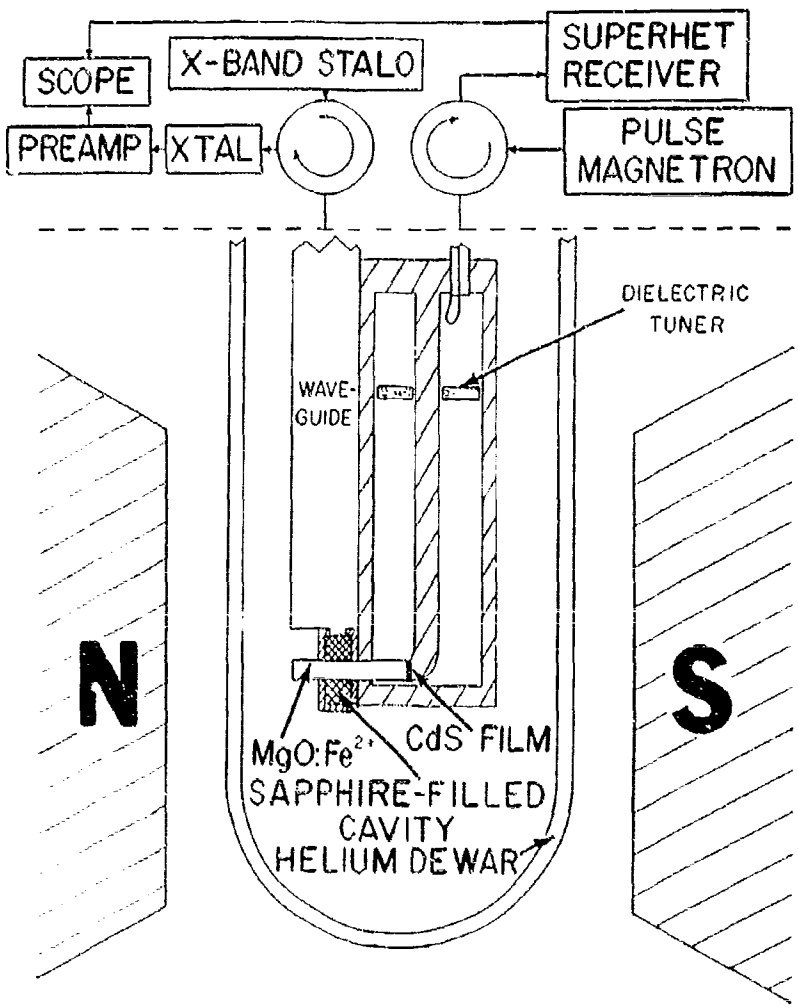

Figure 2. Electronics (top) and experimental apparatus (below the dashed line) used for piezoelectric and double-quantum experiments. Microwave pulses in the 3 to 9 GHz range excite the reentrant cavity. The CdS film transducer in the high-field region of this cavity generates phonons. Each time a phonon pulse passes through the sapphire-filled double-quantum detector cavity, it causes a change in the reflectivity of that cavity, thereby modulating the signal coupled out through the waveguide.

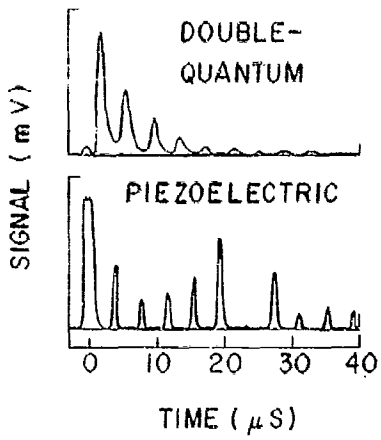

Figure 3. Double-quantum versus piezoelectric detection of successive echoes in the same sample. True energy detection by the double-quantum detector leads to an exponential decay in spite of the nonparallelism of the sample-end faces, and allows more accurate measurement of attenuation.

allowed more precise attenuation measurements. Accuracy in such data will further research in the physical mechanism of attenuation, and therefore in producing delay lines with lower losses.

For the same reason, measurements were also made of the attenuation in different samples of magnesium oxide and correlated with the quality of their crystal structure as measured with a laser ultramicroscope. The difference in attenuation was found to be explainable by defects in the crystals.

Dr. Paul H. Carr is a supervisory research physicist (solid state), and Chief of the Microwave Acoustics Branch, Microwave Physics Laboratory, AFCRL. He received both his B.S. in Physics (1957) and his M.S. in Physics (1961) from M.I.T., and his Ph.D. in Physics (1966) from Brandeis University.

Dr. Carr saw active duty with the Army as a 1st Lt., and was assigned to the Armed Missile Command Calibration Center as a research physicist. There he worked on new techniques for the calibration of accelerometers, infrared and optical detectors, and vacuum gauges. Presently he is making use of microwave phonons for extending the fundamental knowledge of solid-state phenomena, and for use in microwave delay line applications.

Dr. Carr is a member of the American Physical Society, and an associate member of Sigma Xi. He has published widely in the field of microwave acoustics.

Mr. Alan J. Budreau is a research physicist with the Microwave Physics Laboratory, AFCRL. He received his B.S. in Physics from M.I.T. in 1957, and his M.A. from Harvard in 1959. He took an additional year of graduate work at Duke University studying the structure of materials with microwave spectroscopy.

Currently, Mr. Budreau is carrying out research in microwave sound detection. He has several publications to his credit.

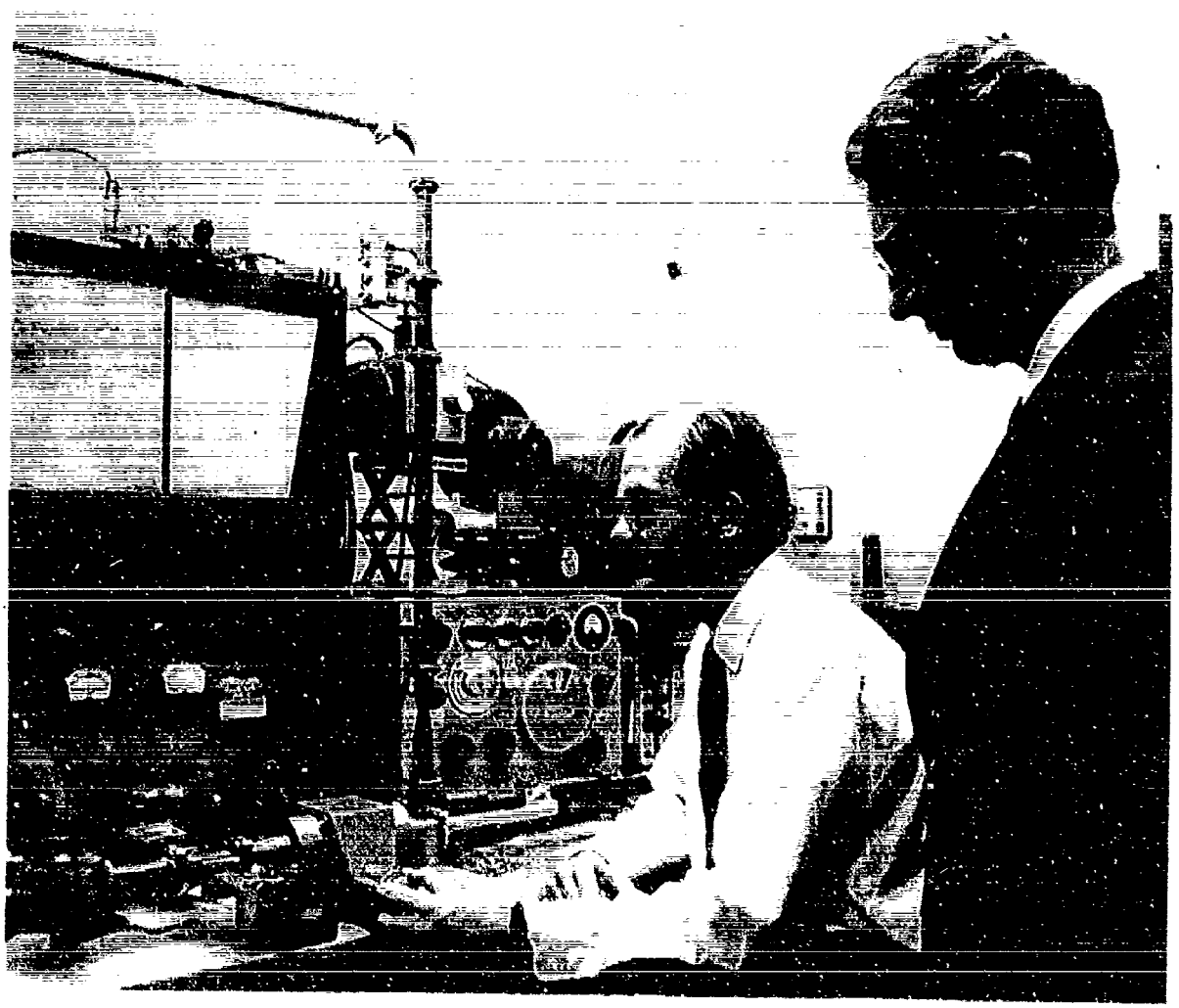

Mr. Alan J. Budreau (left) adjusts the apparatus used for experiments involving sonic delay lines while Dr. Paul H. Carr watches attentively.

TO OUR READERS

Requests for further information should be directed to the individual or laboratory of origin (except for those from Latin America).

Addresses are as follows:

AIR FORCE CAMBRIDGE RESEARCH LABORATORIES
Attn: CRI
Laurence G. Hanscom Field, Bedford, Massachusetts 01730

AEROSPACE RESEARCH LABORATORIES
Attn: ARI
Wright-Patterson Air Force Base, Ohio 45433

AIR FORCE OFFICE OF SCIENTIFIC RESEARCH
Attn: SRGC
1400 Wilson Blvd, Arlington, Va. 22209

THE FRANK J. SEILER RESEARCH LABORATORY
USAF Academy, Colorado 80840

DET. 8(ORA)OAR
Attn: RRR
Holloman Air Force Base, New Mexico 88330

Requests for further information from institutions and individuals in Latin America should be addressed to:

DET. 7 (LAOAR)OAR
U.S. Embassy-Rio
APO New York 09676

Detailed documentary reports may be obtained from:

CLEARINGHOUSE
U.S. Department of Commerce, Springfield, Virginia 22151

DEFENSE DOCUMENTATION CENTER*
Cameron Station, Alexandria, Virginia 22314

*Qualified requesters